INVESTIGATING THE ROLE OF THE PUTATIVE DISULPHIDE BOND WITHIN THE LOOP CONNECTING α4 AND α5 OF THE *Bacillus thuringiensis* Cry4A TOXIN

WALAIRAT PORNWIROON

A THESIS SUBMITTED IN PARTIAL FULLFILLMENT OF
THE REQUIREMENTS FOR THE DEGREE OF
MASTER OF SCIENCE
(MOLECULR GENETICS and GENETIC ENGINEERING)
FACULTY OF GRADUATE STUDIES
MAHIDOL UNIVERSITY
2000

ISBN 974-664-423-8

Thesis
entitled

INVESTIGATING THE ROLE OF THE PUTATIVE DISULPHIDE BOND WITHIN THE LOOP CONNECTING α4 AND α5 OF THE *Bacillus thuringiensis* Cry4A TOXIN

W. Pornwiroon
.....
Ms. Walairat Pornwiroon
Candidate

C. Angsuthanasombat
.....
Asst. Prof. Chanan Angsuthanasombat, Ph.D.
Major-advisor

C. Krittanai
.....
Chartchai Krittanai, Ph.D.
Co-advisor

G. Katzenmeier
.....
Gerd Katzenmeier, Ph.D.
Co-advisor

Liangchai Limlomwongse
.....
Prof. Liangchai Limlomwongse, Ph.D.
Dean
Faculty of Graduate Studies

Prapon Wilairat
.....
Prof. Prapon Wilairat, Ph.D.
Chairman
Master of Science Programme in
Molecular Genetics and Genetic Engineering
Institute of Molecular Biology and
Genetics

Thesis
entitled

INVESTIGATING THE ROLE OF THE PUTATIVE DISULPHIDE BOND WITHIN THE LOOP CONNECTING α4 AND α5 OF THE *Bacillus thuringiensis* Cry4A TOXIN

was submitted to the Faculty of Graduate Studies, Mahidol University

for the degree of Master of Science (Molecular Genetics and Genetic Engineering)

on

June 5, 2000

W. Pornwiroon.
.....
Ms. Walairat Pornwiroon
Candidate

.....
Asst. Prof. Chanan Angsuthanasombat, Ph.D.
Chairman

Sakol Panyim
.....
Prof. Sakol Panyim, Ph.D.
Member

.....
Chartchai Krittanai, Ph.D.
Member

Boonhiang Promdonkoy
.....
Boonhiang Promdonkoy, Ph.D.
Member

.....
Gerd Katzenmeier, Ph.D.
Member

Liangchai Limlomwongse
.....
Prof. Liangchai Limlomwongse, Ph.D.
Dean
Faculty of Graduate Studies

Sakol Panyim
.....
Prof. Sakol Panyim, Ph.D.
Director
Institute of Molecular Biology and Genetics
Mahidol University

ACKNOWLEDGEMENT

I wish to express my sincere thanks to my advisor, Assistant Professor Chanan Angsuthanasombat, for his warm guidance, dedicated efforts, valuable discussion and encouragement thoughout the course of this study and also my co-advisor and oral presentation committees Dr. Gerd Katzenmeier, Dr. Charchai Krittanai, Professor Sakol Panyim and Dr. Boonhiang Promdonkoy.

I am grateful to Panapat Uawithya and Mr. Somphop Leetachewa for his helpful participant.

This study was supported by the Thailand Research Fund's Research Fellowships granted to Professor Sakol Panyim.

I also wish to express my sincere thanks to Professor Prapon Wilairat, Department of Biochemistry, Mahidol University for his helpful advice and comments.

I would like to extend my appreciation to Professor Yasuda, Department of Microbial Genetics, National Institute of Genetics, Japan for his kindly provide the pET24(+) expression vector for this study.

I am also indebted to my friends and all previous/present members of BDG group, and all technicians of the Institute of Molecular Biology and Genetics, Mahidol University who all share any success of this work.

Finally, I would like to express my deepest appreciation to my lovely parent, all members of my family, and all other friends for their patient, encouragement, and patronage. They are deserved to be mentioned as a part of my success.

Walairat Pornwiroon

4136316 MBMG/M : MAJOR: MOLECULAR GENETICS AND GENETIC ENGINEERING; M.Sc (MOLECULAR GENETICS AND GENETIC ENGINEERING)
KEY WORDS : DELTA-ENDOTOXIN, Cry4A, *Bacillus thuringiensis*, DISULPHIDE BOND

WALAIRAT PORNWIROON: INVESTIGATING THE ROLE OF THE PUTATIVE DISULPHIDE BOND WITHIN THE LOOP CONNECTING α4 AND α5 OF THE *Bacillus thuringiensis* Cry4A TOXIN. THESIS ADVISORS: CHANAN ANGSUTHANASOMBAT, Ph.D., CHARTCHAI KRITTANAI, Ph.D., GERD KATZENMEIER, Ph.D. 116 p. ISBN 974-664-423-8

A 3D model of the activated 65-kDa *Bacillus thuringiensis* Cry4A toxin reveals a putative disulphide bond in the loop connecting helices 4 and 5 that may play a role in function of the toxin. In this study, the recombinant plasmid harboring the *cry4A* gene under control of the *tac* promoter together with the *cry4B* regulatory region was constructed and expressed in *Escherichia coli.* Upon solubilization and trypsin digestion, the 130-kDa Cry4A protein was processed into a 47-kDa polypeptide and a ca. 20-kDa fragment composed of α1-α5. SDS-PAGE showed that the 20-kDa fragment treated with β-mercaptoethanol had mobility slower than the untreated protein, indicating the existence of the C192-C199 disulphide bond within the loop connecting α4 and α5 of the Cry4A toxin. To investigate the role in toxicity of this disulphide bond, site-directed mutagenesis was employed to convert either Cys-192 or Cys-199 to alanine in order to eliminate the disulphide bond. Like the wild-type protein, the non-disulphide bridged mutants were highly expressed as inclusion bodies and were structurally stable upon solubilization and trypsin activation. Gel-shift assays have confirmed disappearance of the pre-existent disulphide bond. The larvicidal activity against *Aedes aegypti* of *E. coli* cells expressing either C192A or C199A mutant toxin has approximately the same as the wild-type toxin. Interestingly, the larvicidal activity of the wild-type inclusions were apparently at least 2-fold more toxic than both mutant inclusions, thus suggesting that the disulphide bond within the α4-α5 loop might indeed be involved in the Cry4A toxin mechanism.

4136316 MBMG/M : สาขาวิชา: อณูพันธุศาสตร์และพันธุวิศวกรรมศาสตร์: วท.ม.
(อณูพันธุศาสตร์และพันธุวิศวกรรมศาสตร์)

วไลรัตน์ พรวิรุฬห์: การศึกษาบทบาทความสำคัญของพันธะไดซัลไฟด์ที่คาดว่าเชื่อมต่อเกลียวอัลฟาที่ 4 และ 5 ของโปรตีนสารพิษ Cry4A จาก *Bacillus thuringiensis* (INVESTIGATING THE ROLE OF THE PUTATIVE DISULPHIDE BOND WITHIN THE LOOP CONNECTING α4 AND α5 OF THE *Bacillus thuringiensis* Cry4A TOXIN) คณะกรรมการควบคุมวิทยานิพนธ์: ชนันท์ อังศุธนสมบัติ, Ph.D., ชาติชาย กฤตนัย, Ph.D., GERD KATZENMEIER, Ph.D. 116 หน้า. ISBN 974-664-423-8

โครงสร้างแบบจำลอง 3 มิติในเฉพาะส่วนที่ออกฤทธิ์ได้ขนาด 65 กิโลดาลตัน ของโปรตีนสารพิษ Cry4A แสดงให้เห็นถึงพันธะไดซัลไฟด์ที่คาดว่าอยู่ในส่วนที่เชื่อมต่อระหว่างเกลียวอัลฟาที่ 4 และ 5 ซึ่งอาจจะมีบทบาทต่อหน้าที่ของโปรตีนสารพิษ ในการศึกษานี้ พลาสมิดลูกผสมซึ่งมียีน *cry4A* ภายใต้การควบคุมของ *tac* promoter และส่วนควบคุมการแสดงออกของยีน *cry4B* ได้ถูกสร้างขึ้นและแสดงออกใน *Escherichia coli* จากการละลายและการตัดด้วยเอนไซม์ trypsin พบว่า โปรตีนสารพิษ Cry4A ขนาด 130 กิโลดาลตัน ถูกตัดย่อยเป็นชิ้นโปรตีนขนาด 47 และประมาณ 20 กิโลดาลตัน ซึ่งชิ้นส่วนเล็กประกอบด้วยเกลียวอัลฟาที่ 1 ถึงเกลียวอัลฟาที่ 5 จากการวิเคราะห์ด้วย SDS-PAGE พบว่าในสภาวะที่มี β-mercaptoethanolนั้น ชิ้นโปรตีนขนาด 20 กิโลดาลตันจะเคลื่อนที่ช้ากว่าเมื่อเปรียบเทียบกับในสภาวะที่ไม่มี β-mercaptoethanol ซึ่งชี้ให้เห็นถึงการมีอยู่ของพันธะไดซัลไฟด์ระหว่าง cysteine ตำแหน่งที่ 192 และตำแหน่งที่ 199 ในส่วนที่เชื่อมต่อระหว่างเกลียวอัลฟาที่ 4 และ 5 จากการอาศัยเทคนิคการทำให้เกิดการเปลี่ยนแปลงยีนเฉพาะที่เพื่อศึกษาบทบาทต่อความเป็นพิษของพันธะไดซัลไฟด์ดังกล่าวนี้ ได้เปลี่ยนแปลง cysteine ตำแหน่งที่ 192 และที่ 199 ไปเป็น alanine ซึ่งเมื่อได้แสดงออกใน *E. coli* พบว่าโปรตีนกลายพันธุ์ทั้ง 2 ชนิดถูกสร้างในรูปของก้อนผลึกโปรตีนเหมือนกับโปรตีนต้นแบบ (wild type) และให้ชิ้นส่วนโปรตีนที่เสถียรเมื่อถูกละลายและตัดด้วยเอนไซม์ trypsin นอกจากนี้ผลของการตรวจสอบด้วยวิธี gel-shift ยังยืนยันการหายไปของพันธะไดซัลไฟด์อีกด้วย และเมื่อทดสอบความสามารถในการฆ่าลูกน้ำยุงลาย *Aedes agypti* โดยใช้ *E. coli* ที่สร้างโปรตีนกลายพันธุ์แต่ละชนิดพบว่าโปรตีนกลายพันธุ์ทั้ง 2 ชนิดสามารถฆ่าลูกน้ำยุงได้ใกล้เคียงกับโปรตีนต้นแบบ แต่เมื่อทดสอบความสามารถในการฆ่าลูกน้ำยุงด้วยก้อนผลึกโปรตีน พบว่าโปรตีนต้นแบบสามารถฆ่าลูกน้ำยุงได้มากกว่าโปรตีนกลายพันธุ์อย่างน้อยประมาณ 2 เท่า ผลการวิจัยนี้สรุปได้ว่า พันธะไดซัลไฟด์น่าจะมีบทบาทในกลไกการออกฤทธิ์ของโปรตีนสารพิษ Cry4A

CONTENTS

CONTENTS (CONT.)

CONTENTS (CONT.)

CONTENTS (CONT.)

LIST OF TABLES

LIST OF FIGURES

LIST OF FIGURES (CONT.)

LIST OF ABBREVIATIONS

%(w/v)	percent weight by volume
%(w/w)	percent weight by weight
%C	percent of crosslink
%T	percent of gel
Å	angstrom.
Amp	ampicillin
ATP	adenosine triphosphate
BSA	bovine serum albumin
Bt	*Bacillus thuringiensis*
°C	degree celsius
ca.	approximately
Cry	crystal
CTAB	cetyl trimetyl ammonium bromide
Cyt	cytolytic
dATP	deoxyadenosine-5'-triphosphate
dCTP	deoxycytidine-5'- triphosphate
dGTP	deoxyguanosine-5'- triphosphate
dTTP	deoxythmidine-5'- triphosphate
dNTP	dATP, dCTP, dGTP and dTTP
DNA	deoxyribonucleic acid
DTT	1,4-dithiothreitol

LIST OF ABBREVIATIONS (CONT.)

E. coli	*Escherichia coli*
EDTA	ethylenediamine tetraamino acid
et al.	and others
g	gram (s)
hr(s)	hour (s)
IPTG	isopropyl-β-D-thiogalactopyranoside
kb	kilobase (s)
kDa	kilodalton (s)
LB	Luria-Bertani medium
M	molar
mg	milligram (s)
min	minute (s)
ml	millilitre (s)
mm	millimetre (s)
mM	millimolar
µg	microgram (s)
µl	microlitre (s)
µM	micromolar
µm	micrometre (s)
ng	nanogram (s)
nm	nanometre (s)

LIST OF ABBREVIATIONS (CONT.)

N-terminal	amino terminal
OD	optical density
PCR	polymerase chain reaction
ρmol	picomole
p.s.i.	pound per square inch
RNA	ribonucleic acid
RNase A	ribonuclease A
rpm	revolutions per minute
SDS	sodium dodecyl sulfate
SDS-PAGE	sodium dodecyl sulfate polyacrylamide gel electrophoresis
sec	second (s)
subsp.	subspecies
TEMED	N,N,N',N'-tetramethyl-ethylenediamine
Tris-HCl	Tris-(hydroxymethyl)-aminoethane hydrochloric acid
U	Unit (s)
UTR	untranslated region
UV	ultraviolet
V	volt (s)

CHAPTER I

INTRODUCTION

1. General Background

Bacillus thuringiensis (*Bt*) is a Gram-positive bacterium which produces crystalline inclusions during sporulation. These inclusions are composed of one or more toxic proteins known as insecticidal crystal proteins (ICPs) or δ-endotoxins which are highly toxic to the larvae of major insect crop pests as well as disease vectors (1). Due to their high specificity and safety for the environment, δ-endotoxins are a valuable biological alternative to traditional chemical pesticides (2, 3).

Many of the δ-endotoxin genes have been cloned and sequenced. The cloned proteins were classified into two groups: the Cry (crystal) and Cyt (cytolytic) toxins based on the similarity of their deduced amino acid sequences (3). The Cry toxins (70-140 kDa) are toxic to different species of lepidopteran, coleopteran, dipteran insects (3) and certain parasitic nematodes and protozoan pathogens (4). The Cyt (27-30 kDa) toxins show a wide range of cytolytic activity against insect and mammalian cells *in vitro*, but are toxic to only dipteran larvae *in vivo* (3, 5, 6).

According to insecticidal activity spectrum and deduced amino acid sequence similarlity, the Cry toxins can be classified into four major classes (3) as follows: CryI are toxic to lepidopteran insects, CryII are toxic to lepidopteran and dipteran insects, CryIII are toxic to coleopteran insects and CryIV are toxic to dipteran insects. Since the novel *cry* genes isolated recently have created some problems for this classification

scheme, Crickmore et al. (6) proposed a novel nomenclature based exclusively on amino acid identity. For example, the 130-kDa Cry4A toxin which produced by *Bt* subsp. *israelensis* and specifically toxic to the dipteran *Aedes* sp., *Culex* sp. and *Anopheles* sp. mosquito-larvae (3) is classified as Cry4Aa1. The complete *cry4A* gene sequence has been referred as the genbank accession number of Y00423 (7).

2. Protein Structure of Cry Toxins

Our understanding of how these δ-endotoxins function at the molecular level has increased substantially over the last decade. Over 100 *cry* genes have been cloned and their sequences have been determined (6). From the alignment of complete deduced amino acid sequence of the Cry proteins family, it revealed eight highly conserved blocks. Blocks 1-5 lie on the active toxic core in the amino-terminal half of the toxin and blocks 6-8 lie on the carboxyl-terminal half of the toxin (1) (**Fig. 1**). Because of the structural core composed of five conserved blocks, it was proposed that all Cry toxins will adopt a more or less similar tertiary structure (8). This postulate has been supported by the two published crystal structures of the lepidopteran-specific Cry1Aa and coleopteran-specific Cry3A toxins (8, 9) (**Fig. 2**). Despite the differences in insect specificity and the comparatively low amino acid sequence identity (36%) between the Cry1Aa and Cry3A proteins, their structures show high overall similarity. Both are globular molecules containing three distinct domains. Domain I is a seven α-helix bundle in which the central helix (α5) is relatively hydrophobic and completely surrounded by six other amphipatic helices. This domain has been shown to be responsible for membrane insertion and pore formation (10, 11, 12, 13, 14, 15).

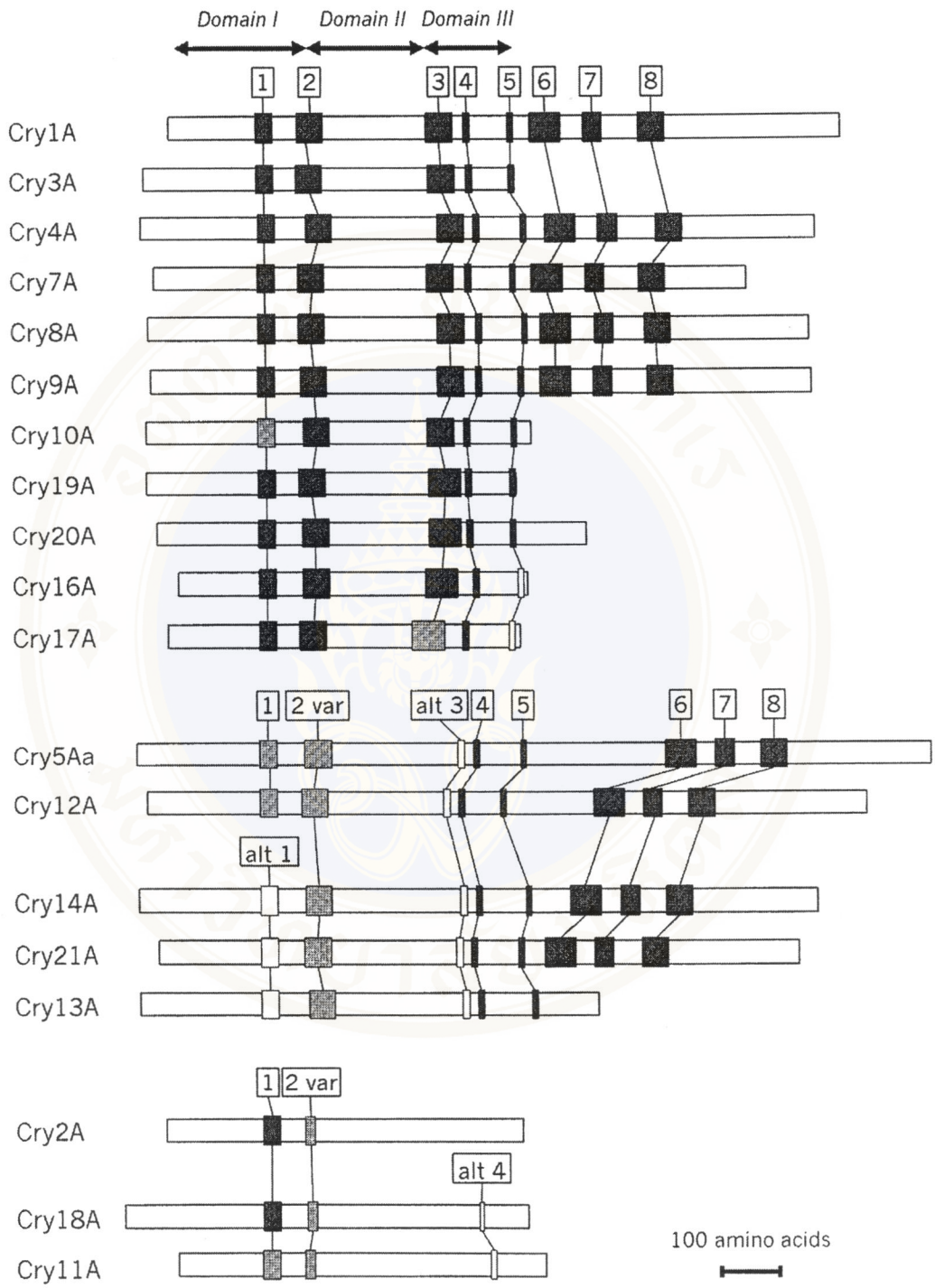

Figure 1 Positions of conserved blocks among Cry Toxins

Sequence blocks are shown as black, gray or white to indicate high, moderate, or low degree of homology, respectively, to the consensus sequence for each conserved block. Variant (var), alternate (alt) (duplicated from ref. 1)

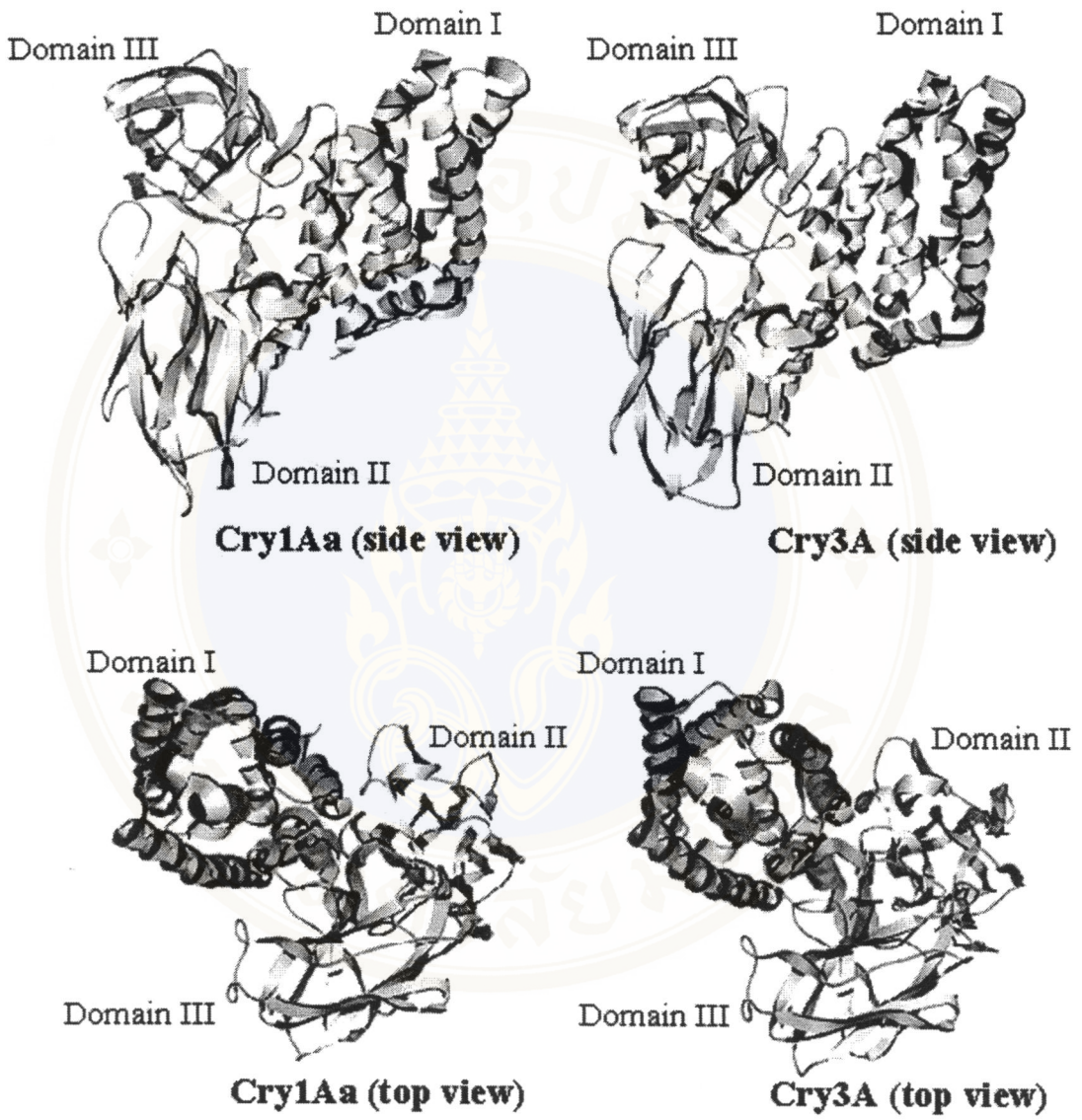

Figure 2 The ribbon structure of Cry1Aa and Cry3A both of top view and side view
The crystal structure of Cry3A and Cry1Aa were clarify by X-ray crystallography in 1991 (8) and 1995 (9) respectively, both compose of three domains.

Domain II, the most divergent part in the two toxin structures, consists of three antiparallel β-sheets containing three surface-exposed loops packed around a hydrophobic core. This domain has been described as the specificity-determining domain, since reciprocal hybrid genes between closely related toxins (Cry1Aa and Cry1Ac) resulted in chimeric toxins with altered specificity (16, 17, 18). Mutation analysis of loop residues in this domain suggested that the loop region is involved in receptor binding (19, 20, 21, 22, 23, 24, 25, 26). Domain III is a β-sandwich of two antiparallel β-sheets. The function of this domain is still in debate although it has been proposed to be involved in either pore formation (27, 28, 29), receptor binding (30, 31, 32, 33, 34, 35, 36, 37, 38, 39) or stabilizing the toxin by protection from proteolysis (8).

Recent study has proposed the plausible three dimensional model for the activated 65-kDa Cry4A δ-endotoxin (40). This structural model was constructed by homology modelling based on the coordinates from the Cry1Aa crystal structure. Like the known structure, the derived structure consists of three domains (I-III): a helical bundle domain (I), a β-prism domain (II) and a β-sandwich (III). Therefore, the proposed model was used in this study.

3. Mechanism of Action of Cry Toxins

3.1 Solubilization and Proteolytic Activation

Bt toxins are naturally present in inclusions as insoluble inactive protoxins. Upon ingestion by the susceptible larvae, the protoxins are solubilized under the alkaline conditions of the insect midgut and proteolytically processed *in vivo* by gut proteases to release the active toxins (3). The toxin activation can be done *in vitro* by digesting the protoxins with larval gut extracts or trypsin (41, 42, 43, 44).

The proteolytic activation of Cry4A with mosquito larval gut extracts showed that the 130-kDa Cry4A protoxin was processed into two protease-resistant fragments of 18-20 and 45-47 kDa through the intramolecular cleavage at the loop connecting α5 and α6 (43).

3.2 Toxin-Receptor Binding

It is believed that the activated toxin binds to the specific receptors on the brush border membrane of midgut epithelial cells (45). The interaction of the toxin with the receptor has been studied extensively with brush border membrane vesicles (BBMV) (23, 24, 25, 33, 36, 37, 39, 45, 46).

So far, two proteins have been identified as specific receptors of the Cry1 toxins The first is aminopeptidase N (APN) isolated from *Manduca sexta, Lymantria dispar, Heliothis virescens* and *Plutella xylostella* that is specific to Cry1Ac (47, 48, 49, 50), and the one isolated from *Bombyx mori* is for Cry1Aa. Another specific receptor is cadherin-like protein which is purified from *M. sexta* and specifically binds to Cry1Ab (51).

3.3 Toxin- Membrane Interaction and Oligomerization

After the toxin binds to the receptor, it is believed that there is a change in the toxin conformation allowing toxin insertion into the membrane. Oligomerization of the toxin occurs to form leakage pores leading to osmotic cell lysis (5).

There are two possible models proposed for the organization of the pore-forming domain of the *Bt* δ-endotoxin within the membrane (5). The first one is a penknife model suggesting that the α5 and α6 joined by the loop at the top of the structure flip out like a penknife opening and insert into the membrane (**Fig.3**). The second model is

an umbrella model which involves the insertion of a helical hairpin α4-α5 into the membrane while the remaining helices spread out on the membrane surface forming an umbrella-like structure (**Fig.4**).

Knowles and Ellar (52) have estimated the pore size formed by Cryl toxins by using sugars and polyethylene glycol molecules of different sizes as osmotic protectants and found that a calculated pore size was between 1 and 2 nm. This measurement suggested that the Cryl pore could be formed by four to six monomers (53).

Feng and Becktel (54) reported that the Cry1Aa and Cry1Ac toxins existed both as monomers and oligomers with apparent molecular masses greater than 220 kDa in solution and that the relative amount of oligomer depended on pH, while Cry3A was found as a monomer at neutral pH. It also suggested that alkaline pH promoted toxin oligomerization.

Guereca and Bravo (55) found that Cry1Aa, Cry1Ac, Cry1C, Cry1D and Cry3A toxins formed an oligomer consisting of more than ten subunits in both neutral and alkaline solution. It suggested that oligomer formation might be a time-dependent process and might occur after the toxin binds to the receptor and inserts into the membrane.

Aronson et al. (56) examined the steps required for toxin insertion into the membrane and possible oligomerization to form a channel. When the Cry1Ab or Cry1Ac toxins were incubated with vesicles from the midguts of *M. sexta* larvae and analyzed by immunoblotting, it was found that most of the toxins formed a large aggregate of ca. 200 kDa. No oligomerization occurred when inactive toxins with mutations in α5 were tested. There was one exception; a very active helix 5 mutant

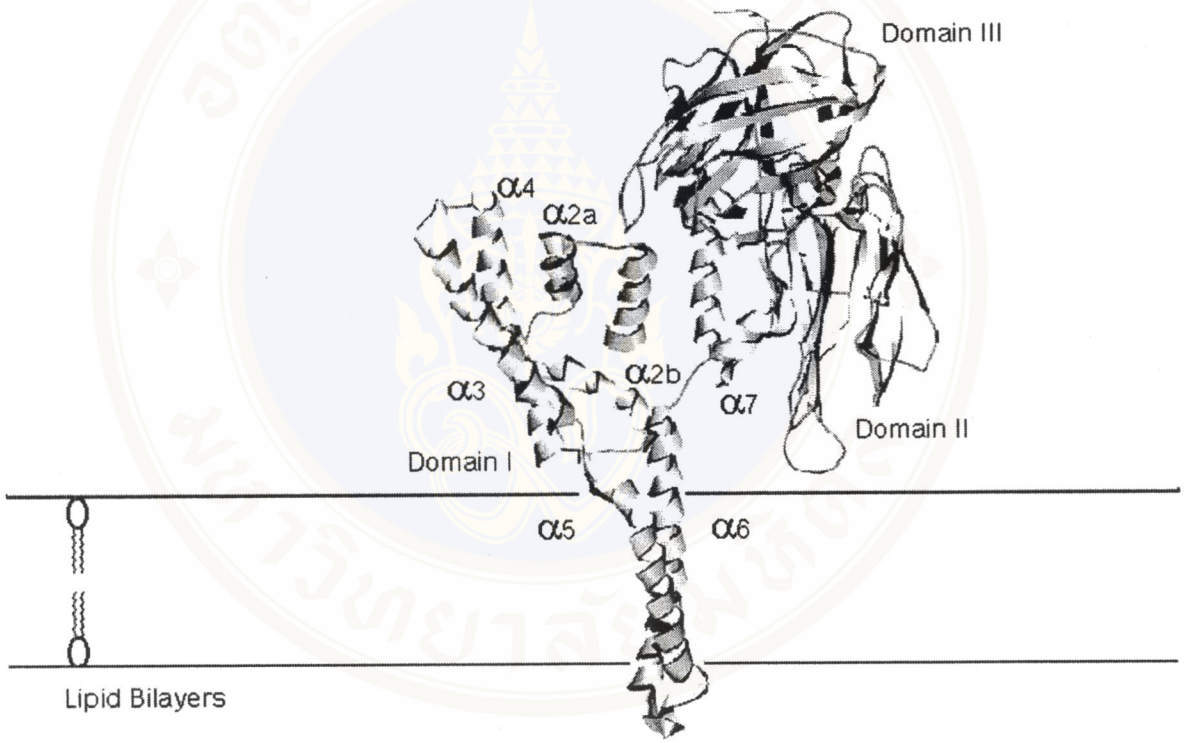

Figure 3 The penknife model

The figure shows the penknife model reproduced from Knowles (5). Helices 5 and 6 flip into the membrane as a helical hairpin.

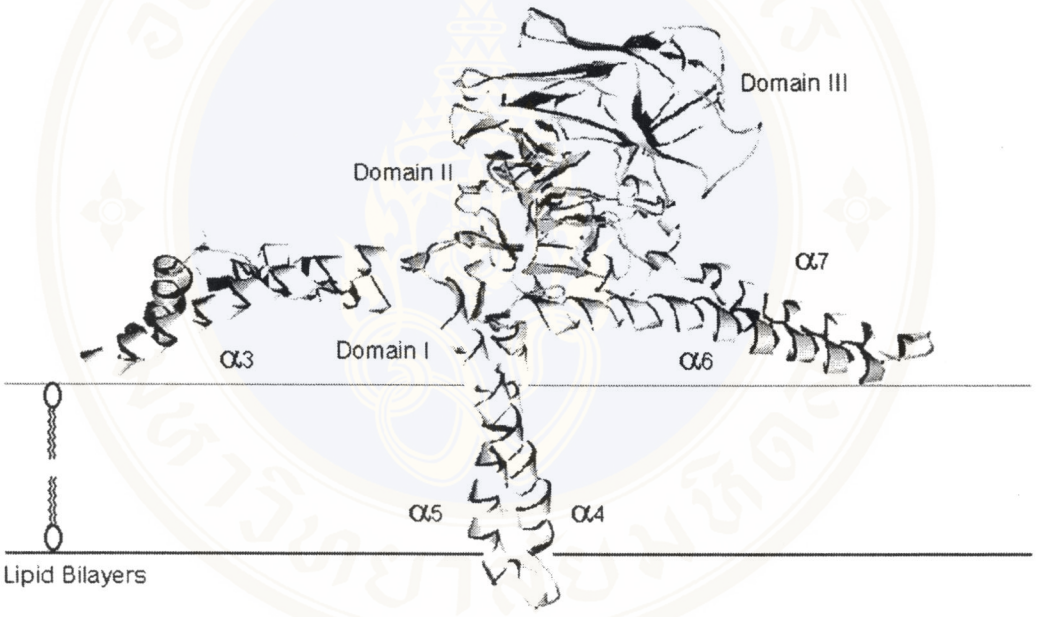

Figure 4 The umbrella model

The proposed pore forming model of *Bt* toxins by insert the hydrophobic hairpin α4 and α5 into the membrane to initiate the pore, while the other helices spread on the surface of membrane like the umbrella ribs.

toxin bound very well to membranes, but no oligomers were detected. Toxins with mutations in the loop connecting α2 and α3, which affected the irreversible binding to vesicles, also did not oligomerize.

3.4 Toxin-Ion Channel

The ion channel activity of Cry toxins has been explored by a wide variety of techniques. Knowles and Ellar (52) reported the effects of Cry toxins on CF-1 cells and proposed the colloidal osmotic lysis model that caused by an influx of water and ions resulting in cell swelling and eventually lysis.

Lorence et al. (57) reported that the Cry1D cationic channel formed in whole *Spodoptera frugiperda* BBMV were blocked by Ba^{2+} and Ca^{2+}. Moreover, Harvey et al. (58) also found that Ba^{2+}, the K^+ channel blocking agent, could completely reverse *Bt* inhibition of the K^+-carried short circuit current in the isolated midgut of *M. sexta*.

Peyronnet et al. (59) measured the effects of different toxins on the electrical potential of the apical membrane of freshly isolated midguts from gypsy moth (*Lymantria dispar*) and silkworm (*Bombyx mori*) larvae with a conventional glass microelectrode and reported that addition of toxins caused a rapid, irreversible, and dose-dependent depolarization of the membrane. It was found that the ability of Cry toxins to form pores in the midgut epithelial cell membrane correlated with their *in vivo* toxicity.

Slatin et al. (60) examined the Cry1Ac and Cry3A in planar lipid bilayer membranes of various compositions and found that toxins formed cation-selective channels. In addition, Schwartz et al. (61) found that Cry1Aa, Cry1Ac and Cry1C

formed at much lower doses channels in the receptor reconstituting planar lipid bilayers than in receptor-free membranes.

Channel formation in planar lipid bilayers has also been observed with N-terminal fragment (essentially domain I which is responsible for ion channel formation) of Cry1Ac (62) and Cry3Bb (63). It was found that the channels formed with Cry1Ac N-terminal fragments differed from those formed by the whole toxins. In contrast, N-terminal fragments of Cry3Bb were quantitatively similar to the full-length toxin.

The role of conserved hydrophobic region located near the N-terminus has been investigated by site directed mutagenesis. Wu and Aronson, (11) reported that Ala-92 and Arg-93 mutations in α5 of Cry1Ac resulted in loss of toxicity, suggesting that the amphipatic helical region of the toxin was essential for toxicity. The mutant toxins had lost the capacity to inhibit K^+-dependent amino acid transport into larval midgut vesicles, but there was no effect on their ability to compete with wild type toxin for binding. Chen et al. (12) also found that A92E and Y153D mutation of Cry1Ab resulted in loss of toxicity. Moreover, reduction of pore function as tested by voltage clamping and irreversible binding of these two mutant toxins to *M. sexta* brush border membrane vesicles was observed.

Through the disulfide bridge mutation in domain I of Cry1Aa, Schwartz et al. (14) demonstrated that the domain was involved in membrane integration and permeation. They showed that unfolding of the protein around a hinge region linking domain I and II was a necessary step for pore formation. They also suggested that membrane insertion of the hydrophobic helical hairpin α4 and α5 played a critical role in the formation of a functional pore. The proposal was supported by Uawithya et al. (64) when they

performed single proline substitution on α3 and α4. They reported that helix 4 of the Cry4B toxin could possibly involved in the membrane insertion and pore formation rather than in receptor recognition. Manoj Kumar and Aronson (65) performed either random mutagenesis of thirty-nucleotide segments in *cry1Ac1* gene, encoding parts of α4 and the loop connecting α4 and α5 or site-directed mutagenesis of specific surface residues in α3. They found that 12 random mutations in α4 and α5 resulted in the total loss of toxicity. Mutation either in the loop connecting α4 and α5 or in α3 did not affect toxicity. In contrast to mutations in α5, those in α4 which inactivated the toxin did not affect its capacity to oligomerize in the membrane, but there was no ion flow as measure by light scattering. They also suggested that α5 is important for oligomerization and perhaps has other functions, whereas α4 must have a more direct role in establishing the properties of the channel.

Some of amphipathic helices were studied by using synthetic peptides as the model. A synthetic 31-mer peptide corresponding to the sequence of the central helix (α5) of CrylAc was structurally and functionally characterized by Cummings et al. (66). They found that the peptide could exist as an alpha helix in methanol and as a random coil in water. In addition, the peptide could associated with liposomes and formed channels in planar lipid bilayers.

Gazit and Shai (67) synthesized the peptide corresponding to the α5 segment, amino acid residues 193-215 of Cry3A and its proline incorporated analogue (P-α5), and selectively labeled at their N-terminal amino acids with fluorescent probes. It was reported that α5 was much more active than P-α5. The same approach was used in characterization of the ability to self-assemble and to co-assemble within lipid

membranes of α5 and α7 (68). It was revealed that, in their membrane-bound state, α5 could self-associate but α7 could not, and that α5 could coassemble with α7 but not with an unrelated membrane bound α-helical peptide.

Gazit et al. (69) also investigated the role of α5 with respect to its interaction with Sf-9 cell membranes and its propensity to form ion channels in planar lipid membranes. Functional characterization of α5 has revealed that it was cytotoxic to Sf-9 insect cells, and could form ion channels in planar lipid membranes. Moreover a proline-substituted analogue of α5 was less cytolytic and slightly more exposed to enzymatic digestion. These findings would support a role for α5 in the mechanism of the delta-endotoxins, as one of the transmembrane helices to form the toxic pore.

Gazit et al. (15) have used resonance energy transfer measurements of all possible combinatorial pairs of membrane-bound helices to map the network of interactions between helices in their membrane-bound state. It was proposed that α4 and α5 would insert into the membrane as a helical hairpin in an antiparallel manner, while the other helices would lie on the membrane surface like the ribs of an umbrella (the "umbrella model"). They also suggested that α7 may serve as a binding sensor to initiate the structural rearrangement of the pore-forming domain.

CHAPTER II

OBJECTIVES

Although the structure of the Cry toxins have provided some insights into the possible steps that lead to cell death, the identity of the membrane-inserting components in ion channel formation is still not clear. Several studies with the isolated domain I of Cry1Ac (62) and Cry3Bb (63) and synthetic peptides of helix-5 from Cry1Ac (66), Cry3A (67, 68) have demonstrated pore forming activity in phospholipid bilayers. Directed mutagenesis studies by introducing disulphide bridges into the Cry1Aa toxin suggested that membrane insertion of the helical hairpin α4 and α5 played a critical role in the formation of a functional pore (14). Studies in α3 and α4 of the Cry4B toxin by proline substitution mutagenesis showed that helix 4 is involved in membrane insertion and pore formation rather than in receptor recognition (64). Furthermore, random mutation in helix 4 and helix 5 of Cry1Ac1 toxin suggested that helix 4 must have a role in establishing the properties of the channel (65).

Recent studies have proposed the plausible three dimensional model for the activated 65-kDa Cry4A δ-endotoxin (40). This structural model was constructed by homology modelling based on the coordinates from the Cry1Aa crystal structure. Like the known structure, the derived structure consists of three domains (I-III): a helical bundle domain (I), a β-prism domain (II) and a β-sandwich domain (III) (**Fig. 5**). Structural analysis of the model has revealed a putative disulphide bond (C192-C199) within the loop connecting α4 and α5. This disulphide bond may play a role in toxin

mechanism, possibly in membrane insertion of the helical hairpin α4-α5 of the Cry4A toxin.

In this study it was aimed to investigate the role in toxicity of the putative disulphide bond within the loop connecting α4 and α5 of the Cry4A toxin.

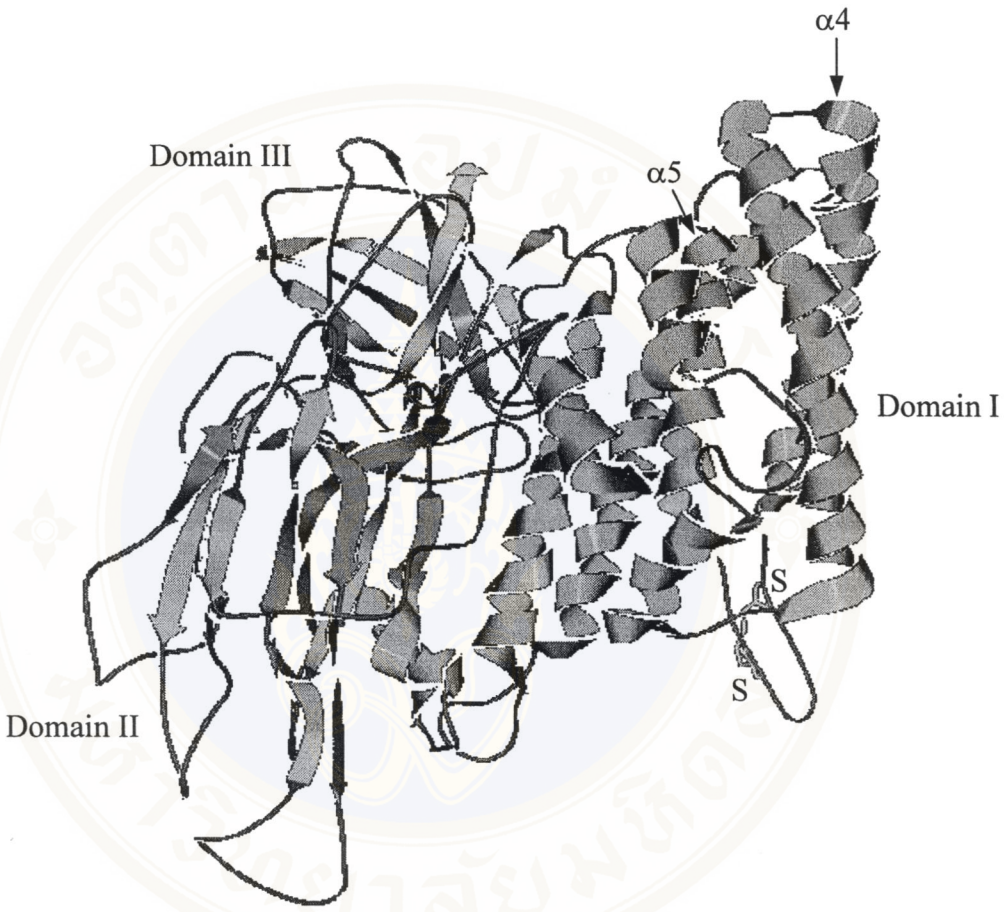

Figure 5 Ribbon model of the activated 65-kDa Cry4A toxin

The figure shows the organization of three domains (I-III) and the putative disulphide bond (S-S) between C192 and C199 within the loop connecting α4 and α5 of the activated 65-kDa Cry4A toxin which constructed by homology modelling (40).

CHAPTER III

MATERIALS

1. Chemicals

Adenosine triphosphate (ATP)	Gibco BRL
Cetyl trimethyl ammonium bromide (CTAB)	Sigma
Coomassie brilliant blue R-250	Sigma
1,4-dithiothreitol (DTT)	Sigma
β-mercaptoethanol	Sigma
Isopropyl-β-D-thiogalactopyranoside (IPTG)	Sigma

Other chemicals and solvents used were purchased from various suppliers (BIO-RAD, Fulka, Merck and Sigma).

2. Enzymes and Accessory Buffers

All enzymes used were purchased from Gibco BRL, New England Biolabs and Promega. The accessory buffers were supplied by the enzyme manufacturer.

3. Bacterial Strains

E. coli strain JM109 [*recA*1 *supE*44 *endA*1 *hsdR*17 *gyrA*96 *rclA*1 *thi*Δ(*lac-proAB*) F' (*traD*36 *proAB*$^{+}$ *lacI*^{q} lacZ ΔM15)] was purchased from Promega.

E. coli strain BL21(DE3)pLysS [F^- *ompT hsdS*$_B$ (r_B^-, m_B^-) *gal dcm* (DE3)pLysS (Cm^R)] was purchased from Stratagene.

4. Vectors and Recombinant Plasmids

pBA (70) (see **Fig. 6)** : a recombinant plasmid containing the 130 kDa Cry4A toxin gene under control of the *cry4B* regulatory region and the *LacZ* promoter (Genbank accession number : Y00423)

pMEx8 (71) (see **Fig. 7)** : an expression vector containing the *tac* promoter designed to express a gene of interest

pET 24(+) (see **Fig. 8)** : an expression vector (Novagen's product) containing the T7 promoter designed to express a gene of interest, kindly provided by Professor S.Yasuda (Department of Microbial Genetics, National Institute of Genetics, Japan).

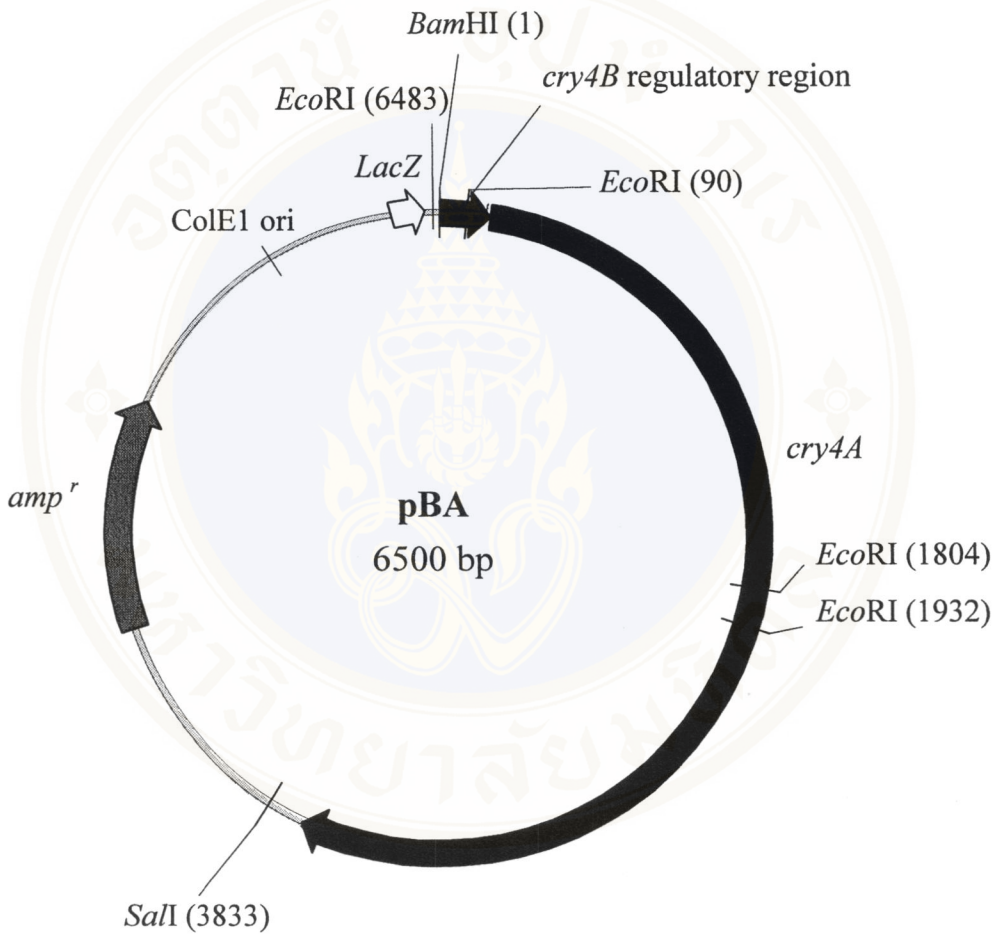

Figure 6 Physical map of the recombinant plasmid pBA (70)

The figure illustrates the recombinant plasmid pBA containing the 130 kDa Cry4A toxin gene under control of the *cry4B* regulatory region and the *LacZ* promoter.

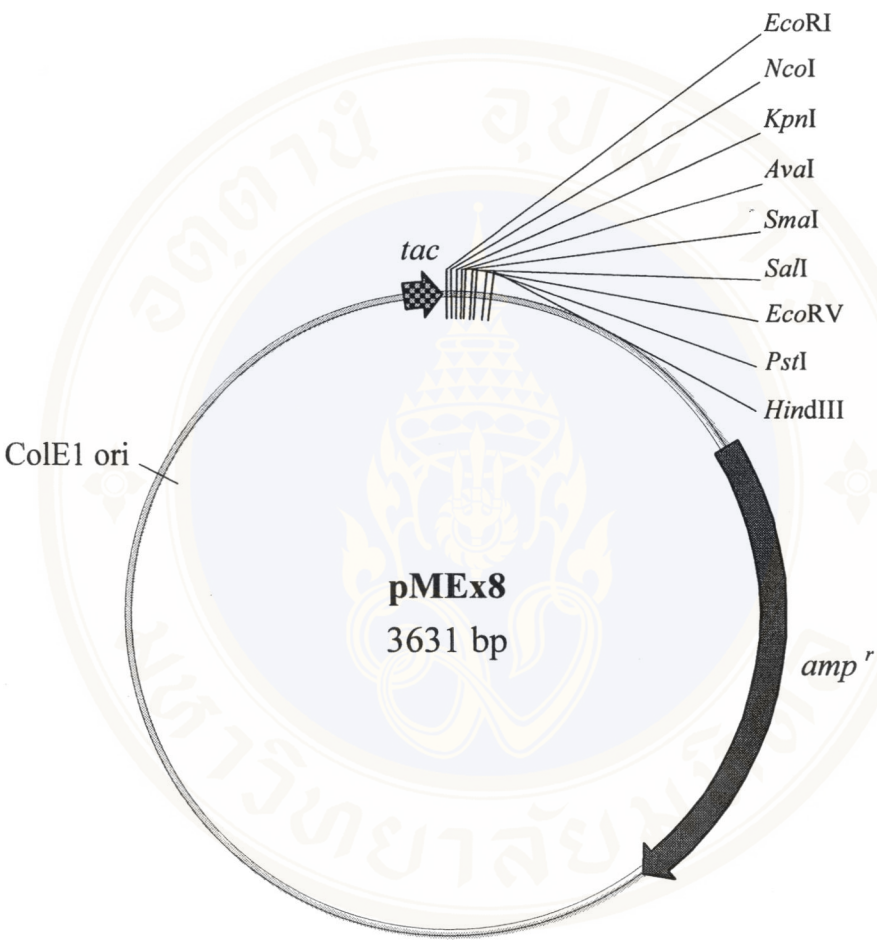

Figure 7 Physical map of the plasmid pMEx8 (71)

The figure illustrates the plasmid pMEx8 containing *tac* promoter, multiple cloning sites, ColE1 origin of replication and ampicillin resistance gene.

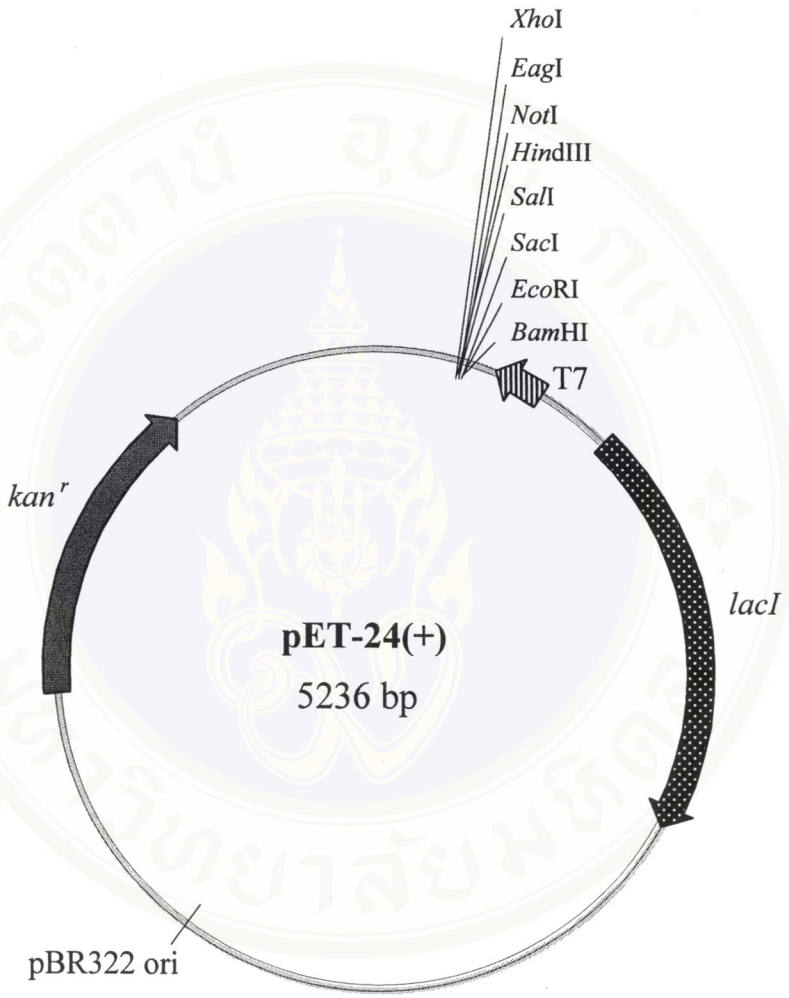

Figure 8 Physical map of the plasmid pET24(+)

The figure illustrates the plasmid pET24(+) containing T7 promoter, multiple cloning sites, pBR322 origin of replication, *lacI* gene and kanamycin resistance gene.

5. Synthetic Oligonucleotides (Primers)

Synthetic oligonucleotides served as primers in PCR were synthesized by Bio-synthesis, U.S.A. for C192A-f, C192A-r, C199A-f and C199A-r. It is also by oligonucleotide synthesis division of Central Equipment Laboratory, Mahidol University for 4AUTR(-)-f and 4AUTR(-)-r. The oligonucleotide sequences are shown as follows. The mutated nucleotide or amino acid residues are in bold type. The introduced restriction enzyme recognition site are underlined. Deduced amino acid sequences are shown above forward primer sequences.

Set 1. PCR primers were used to introduce the additional *Bam*HI and *Hin*dIII recognition sites into cry4B-5'UTR.

4AUTR(-)-f: 5′ CCAGAAAAAG**C**TTG**G**ATCCAATGTGAATATGG 3′

4AUTR(-)-r: 5′ CCATATTCACATTGGAT**C**CAA**G**CTTTTTCTGG 3′

BamHI *Hin*dIII

Set 2. PCR primers were used to substitute cysteine-192 with alanine and introduce *Eco*RI recognition site for screening the mutant plasmid.

P E L V N S **A** P P N

C192A-f: 5′ CCAGAGCTTGT**G**AA**T**TC**TG**CTCCTCCTAATCC 3′

C192A-r: 5′ GGATTAGGAGGAG**CA**GA**A**TT**C**ACAAGCTCTGG 3′

*Eco*RI

Set 3. PCR primers were used to substitute cysteine-199 with alanine and introduce *Ava*I recognition site for screening the mutant plasmid.

```
                    P  P  N  P  S  D  A  D  Y  Y  N
C199A-f:    5′ CCTCCTAACCCGAGTGATGCTGATTACTATAAC 3′
C199A-r:    5′ GTTATAGTAATCAGCATCACTCGGGTTAGGAGG 3′
                                      AvaI
```

6. Culture media

LB broth (72) : 1% bacto-tryptone, 0.5% yeast extract, 1% NaCl

7. Miscellaneous

Ampicillin	Sigma
Kanamycin	Sigma
Chloramphenicol	Sigma
Deoxyribonucleotide triphosphates (dNTP)	Promega
GENECLEAN II kit	Bio 101 Inc.
Standard DNA Marker	Gibco BRL, Biolabs
BIO-RAD Protein Assay	BIO-RAD
SDS-PAGE molecular weight standards, broad range	BIO-RAD

CHAPTER IV

METHODS

1. Plasmid DNA Extraction Using the CTAB Method (73)

A single colony of bacteria was inoculated into 3 ml LB broth with an appropriate amount of antibiotic and incubated at 37°C with 200 rpm shaking for 16-20 hrs. Overnight culture was transferred into 1.5 ml microcentrifuge tube and centrifuged at 10,000 rpm for 10 sec. Supernatant was discarded and resuspended cell pellet in 200 µl of STET buffer (8% sucrose, 50 mM Tris-HCl pH 8.0, 50 mM EDTA and 0.1% Triton-X 100). A volume of 10 µl of freshly prepared lysozyme solution (10 mg/ml) was added and incubated at room temperature for 20 min. The mixture was boiled for 30-45 sec and immediately centrifuged at 12,000 rpm for 15 min at room temperature. The pellet (chromosomal DNA) was removed with a sterile toothpick. Plasmid DNA and residual low molecular weight RNA were recovered from the supernatant by adding 1/10 volume of 5% CTAB. The tubes were inverted 5-6 times, incubated at room temperature for 30 min and centrifuged at 12,000 rpm for 10 min at room temperature. The pellet was resuspended in 300 µl of 1.2 M NaCl by vigorous vortexing and 10 µl of RNase A solution (10 mg/ml) was added to remove RNA and incubated at 37°C for 30 min. The protein was removed by adding 300 µl of chloroform, mixed by inversion for 30 sec and centrifuged at 12,000 rpm for 5 min at room temperature. The clear aqueous phase was transferred to a new tube. The DNA

pellets were precipitated with 2 volumes of absolute ethanol at –20°C for 5 min and centrifuged at 12,000 rpm for 15 min at room temperature. The DNA pellets were washed with 70% ethanol, dried and resuspended in 20 µl of sterile distilled water.

2. Restriction Endonuclease Digestion of Plasmid DNA (72)

In 20 µl digestion reaction, 0.2-1 µg of plasmid DNA, 1x restriction enzyme digestion buffer, and approximately 5 U of restriction endonuclease and sterile distilled water to make up the 20 µl total volume were mixed together and incubated at a specific temperature for a period of time depending on the specification supplied by the enzyme manufacturer.

3. Agarose Gel Electrophoresis of DNA (72)

To analyze the size or restriction pattern of DNA sample, the sample was subjected to agarose gel electrophoresis as described by Sambrook et al. (72). The appropriate amount of agarose powder (Prona) was dissolved in 1xTBE buffer [90 mM Tris, 90 mM boric acid, 2 mM EDTA (pH 8.0)] under boiling temperature to insure the homogeneity of gel solution. When the gel mixture cooled down to about 60°C, the mixture was poured into the mold and allowed to cool and to solidify at room temperature. DNA sample solution was mixed with gel-loading dye [15% (w/v) Ficoll 400, 0.01% (w/v) Bromophenol blue] at ratio 1:5 and loaded into the well of the gel.

The electrophoresis was performed at constant voltage of 100 V in the same buffer that was used to prepare the gel. After the electrophoresis was completed, the gel was stained in 0.5 µg/ml ethidium bromide solution for 5-10 min and then

destained in single distilled water for 10-15 min. The DNA band was visualized under UV.

4. Purification of DNA fragment by GENECLEAN II kit

GENECLEAN II Kit (BIO101) can be efficiently used to purify the DNA fragment of 0.5-15 kb in length. The 1xTAE buffer [0.04 M Tris-acetate, 0.001 M EDTA (pH 8.0)] was used in gel electrophoresis of DNA separation instead of TBE buffer. The desired DNA band was quickly excised from the gel under long-wavelength UV light and transferred to the eppendorf tube. NaI solution was added as 3 volume per 1 volume of gel slice (e.g. 300 µl per 0.1 g of gel slice). The agarose was dissolved by incubating at 55°C for 5 min while mixing every minute by inversion. The glassmilk suspension was mixed thoroughly by vortexing and 5 µl of the suspension was added to the solution containing 5 µg or less of DNA. An additional 1 µl of glassmilk suspension was added for each of 0.5 µg of DNA above 5 µg. The mixture was placed on ice for 30 min while mixing gently by inversion to allow binding DNA to the silica matrix. The pellet of glassmilk-DNA complex was collected by 5 sec centrifugation at maximum speed in a microcentrifuge. The supernatant was removed and then centrifuged again. The rest of NaI solution was removed by pipetting. The pellet was washed 3 times with New Wash solution by using 200 µl in the first wash and 400 µl in the next 2 washes. After the third wash, all the New Wash solution was removed from pellet by centrifugation. The DNA was eluted twice by resuspending the pellet in the equal volume of TE buffer (10 mM Tris-HCl pH 8.0, 1 mM EDTA pH 8.0) or sterile distilled water, incubated at 55°C for 2 min and centrifuged at maximum speed

in a microcentrifuge for 30 sec. The DNA solution was transferred to the new microcentrifuge tube.

5. Fill-in of Restricted DNA Termini (72)

The purified sticky ended DNA fragments were mixed with 1x T_4 DNA Polymerase buffer, 100 μM of each dNTP, 50 μg/ml of BSA and 1-3 units of T_4 DNA Polymerase (NEB) and incubated at 12°C for 20 min. The reaction was terminated by heating at 75°C for 10 min.

6. DNA Ligation (72)

The vector and insert were ligated at the molar ratio 1:3 in the reaction mixture (50 mM Tris-HCl pH 7.6, 10 mM $MgCl_2$, 1 mM ATP, 1 mM dithiothreitol, 5% (w/v) polyethylene glycol-8,000). One unit of low-concentrated T_4 DNA Ligase (1 unit/μl) (Gibco BRL) was added to the mixture. The reactions were mixed, centrifuged briefly and incubated overnight at 14°C.

7. Preparation of Competent Cells (72)

A single colony of either *E. coli* strain JM109 or *E. coli* strain BL21(DE3)pLysS was inoculated into 3 ml of LB broth and LB broth with 34 μg/ml of chloramphenicol, respectively and cultured at 37°C with 200 rpm shaking for 16-20 hrs. 1 ml of overnight culture was transferred into 100 ml of fresh LB broth and incubated at 37°C with 200 rpm shaking until OD_{600} ~ 0.3-0.5. The cell culture was chilled on ice for 15 min and centrifuged at 3,000 rpm for 10 min at 4°C. The pellet was gently

resuspended twice in 20 ml of cold 0.1 M $CaCl_2$, incubated on ice for 30 min and then centrifuged at 3,000 rpm for 15 min at 4°C. The *E. coli* pellet was gently resuspended in 4 ml of cold 0.1 M $CaCl_2$ and incubated on ice for 15 min. 1.8 ml of glycerol was added into the cell suspension (30% final concentration) and 200 µl aliquots were kept at –80°C until required.

8. Transformation of Competent Cells (72)

An aliquot of 200 µl of competent *E. coli* was mixed with the solution of DNA to be transformed. The cells were incubated on ice for 30 min, followed by incubation at 42°C for 90 sec, and then immediately chilled on ice for additional 5 min. 800 µl of 37°C LB broth were added to the transformed cells, mixed and incubated at 37°C for 1 hr. with shaking at 200 rpm. The transformed cells were pelleted by centrifugation at 6,000 rpm for 1 min. The cells were spread on a LB agar plate containing an appropriate amount of antibiotic and incubated at 37°C for 16 hrs.

9. *In vitro* site directed mutagenesis

The basic procedure based on Stratagene's QuickChange™ Site-directed Mutagenesis Kit (see **Fig. 9**) which basically utilizes a supercoiled, double-stranded DNA (dsDNA) vector with a gene of interest and two synthetic oligonucleotide primers containing the desired mutation. The mutagenic primers, each complementary to opposite strands of the vector, extend during temperature cycling by means of *Pfu* DNA Polymerase which replicates both plasmid strands with high fidelity and without displacing the mutant oligonucleotide primers. Upon incorporation of the primers, a mutated plasmid containing staggered nicks is generated. Following temperature

cycling, the PCR product is treated with *Dpn*I to digest the parental DNA template and to select for mutation-containing synthesized DNA since this endonuclease is specific for methylated and hemimethylated DNA (5'-$G^{me}A\downarrow TC$-3'). DNA isolated from almost all *E. coli* strains is *dam* methylated and therefore susceptible to *Dpn*I digestion. The nicked vector DNA corporating the desired mutation is then transformed into *E. coli* competent cells.

10. Setting up the Polymerase Chain Reactions

The PCR was performed by Gene Amp System 2400 (Perkin Elmer Cetus) for controlled incubation of PCR-samples. The PCR reaction mixture (50 µl) composes of 50 µM of each dNTP (dATP, dCTP, dGTP and dTTP), 30 ρmol of each primer, 100 ng of template DNA (pMEx-B4A), 2x reaction buffer (200 mM Tris-HCl pH 8.8, 100 mM KCl, 100 mM $(NH_4)_2SO_4$, 20 mM M_gSO_4, 1mg/ml nuclease-free BSA, and 1% Triton X-100) and double distilled water to a final volume of 50 µl. Before starting the reaction, 3 units of *Pfu* DNA Polymerase was added to the mixture. After the amplification reaction was finished, the PCR products were examined on 0.8% agarose gel electrophoresis.

11. Digesting the PCR products

1 µl of *Dpn*I restriction endonuclease was added to the PCR product and incubated at 37°C for 1 hr. The *Dpn*I will digest the parental *i.e.* nonmutated methylated or hemimethylated dsDNA. Then, the *Dpn*I digested PCR products were analysed on 0.8% agarose gel electrophoresis.

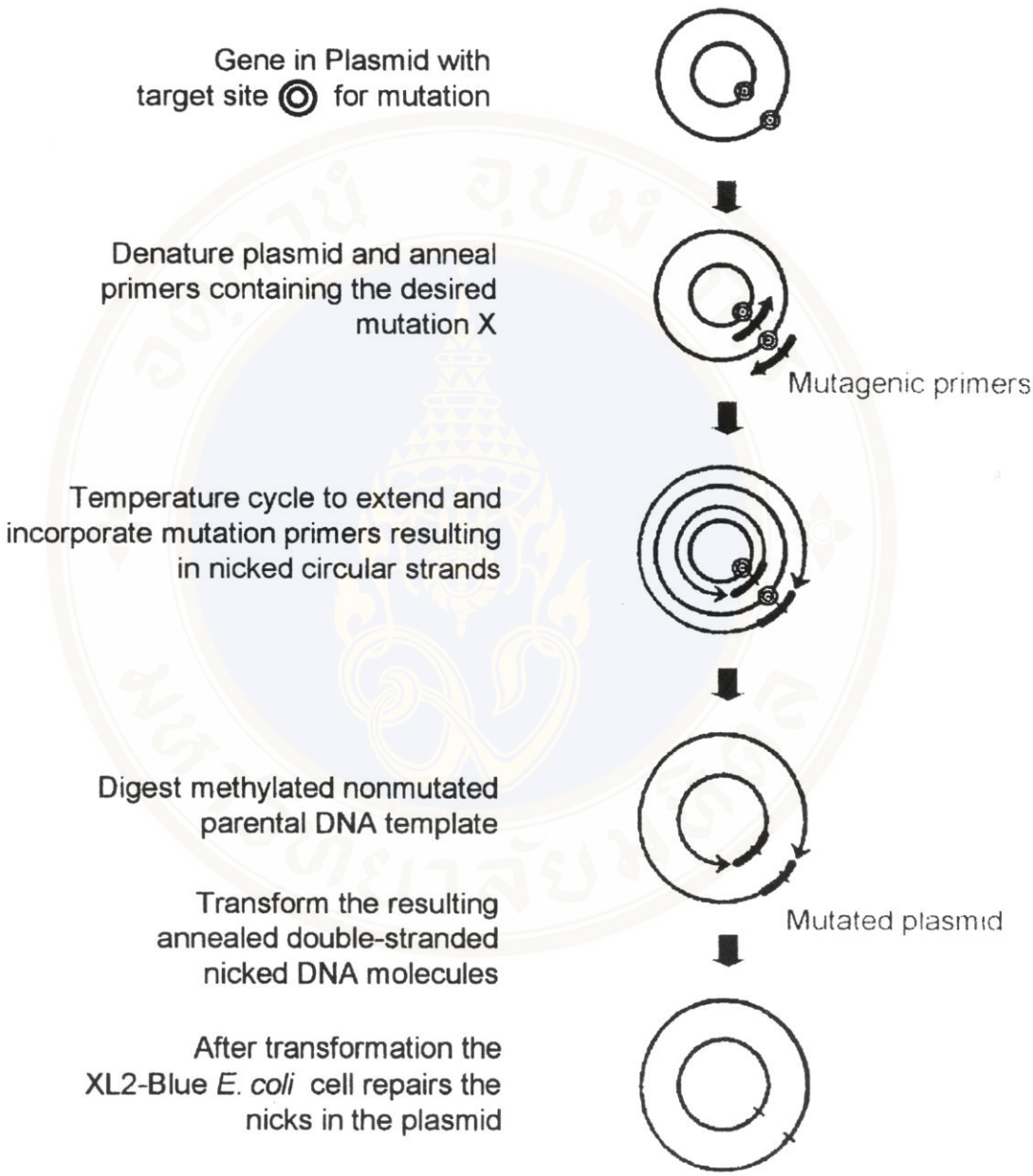

Figure 9 Overview of the QuickChange site-directed mutagenesis method (redrawn from Stratagene's QuickChange™ instruction manual)

12. Expression of Toxins (72)

Each clone of *E. coli* strain BL21(DE3)pLysS carrying the pET-recombinant plasmid expressing the Cry4A wild type toxin was inoculated into 3 ml of LB broth containing 25 μg/ml of kanamycin and 34 μg/ml of chloramphemicol and grown at 37°C and 200 rpm agitation for 16 hrs. One percentage of the overnight culture was inoculated into fresh LB broth containing kanamycin and chloramphemicol and grown until OD_{600} ~ 0.5-0.6. Subsequently, the expression was induced with IPTG at a final concentration of 1 mM at 37°C for 2 and 4 hrs.

Each clone of *E. coli* strain JM109 harboring either the recombinant plasmid (pBA, pMEx-B4A) expressing the Cry4A wild type toxin or the mutant plasmid (pC192A, pC199A) expressing the mutant toxins was inoculated into 3 ml of LB broth with 100 μg/ml of ampicillin and grown at 37°C and 200 rpm agitation for 16 hrs. One percentage of the overnight culture was inoculated into new LB broth with ampicillin and grown until OD_{600} ~ 0.3-0.5. Then, the expression was induced with IPTG at a final concentration of 0.1 mM at either 37°C for 2,4 and 6 hrs or 30°C for 10 hrs.

The culture containing a number of cells equal to 10^8 cells (1 OD_{600} ~ 10^8 cells) were collected by centrifugation at 5000 rpm for 10 min. The total *E. coli* protein was analysed on 10% SDS polyacrylamide gel.

13. Electrophoresis of Protein

13.1 Sample Preparation (74)

Protein samples were mixed with 4x sample buffer [60 mM Tris-HCl (pH 7.5), 2%(w/v) SDS, 10% glycerol, 0.015%(w/v) Bromophenol blue and 100 mM DTT] and

heated at 95°C for 5 min. The heated samples were vigorously vortex mixed and centrifuged at 10,000 rpm for 10 min. The supernatant equal to 0.1 OD_{600} was loaded onto the well of 10% SDS polyacrylamide gel.

13.2 SDS polyacrylamide gel electrophoresis (SDS-PAGE) (75)

SDS-PAGE was carried out using the Bio-Rad Mini-Protein II system. SDS polyacrylamide gel is composed of separating and stacking gel. The separating gel consisted of 2.6%C, 10% or 13%T, 0.375 M Tris-HCl (pH 8.8), and 0.1% SDS. The stacking gel contained of 2.6%C, 6%T, 0.125 M Tris-HCl (pH 6.8), and 0.1% SDS. The gel was run in Tris-glycine buffer (25 mM Tris, 192 mM glycine, and 0.1% SDS). Electrophoresis was performed with constant voltage of 100 V at room temperature.

After electrophoresis, the protein band was visualized by soaking the gel in staining solution (50% methanol, 10% glacial acetic acid and 0.1% Coomassie Brilliant Blue R-250 in water) for 2 hrs. The gel was then soaked in destaining solution (10% methanol and 10% glacial acetic acid) overnight or until the background was clear.

14. Partial purification of Inclusions (76)

E. coli cells expressing the recombinant protein were harvested by centrifugation at 6,000 rpm, 4°C for 10 min. The cell pellets were resuspended in cold distilled water. The cell suspension was lysed in a French Pressure Cell at 900 psi. The cell lysate was centrifuged at 8000 rpm, 4°C for 15 min. The supernatant to be analysed was collected and the inclusions were washed twice in cold distilled water, sonicated at amplitude 2 (3 sec on and 2 sec off for 15 sec) and centrifuged at 10,000 rpm, 4°C for 15 min. The

equal volume of the cell lysate, partial-purified inclusions and supernatant were analysed on 10% SDS polyacrylamide gel.

15. Protein Quantification

Protein concentrations of partial-purified inclusions were determined by using Bio-Rad Protein microassay reagent following the Bradford Method (77). The calibration curve was constructed using bovine serum albumin (BSA) as a protein standard. To prepare the standard protein samples, BSA was diluted into 5 concentrations containing 2, 4, 6, 8 and 10 μg in 800 μl of distilled water. The sample solution in 800 μl was mixed with 200 μl of dye reagent and incubated 10 min at room temperature. The absorbance of samples and standards were measured at 595nm using Hitachi U-2000 Spectrophotometer. The protein concentrations of samples were calculated from the standard curve.

16. Biochemical Characterization of Toxins

16.1 Solubilization and Proteolytic Activation (43)

One mg of protoxin inclusions were solubilized in 1 ml of 50 mM Na_2CO_3, pH 9.0 and incubated at 37°C for 1 hr. For solubility determination, the incubated toxins were subjected to centrifugation at 10,000 rpm for 10 min. Prior-and post-centrifugation toxin samples were quantified as described in **METHOD 15**. Furthermore, the samples were analysed on 10% SDS polyacrylamide gel. For proteolytic activation, the solubilized protoxins were digested with trypsin (N-Tosyl-L-Phenylalanine Chloromethyl Ketone treated, Sigma) at a trypsin: protoxin ratio of 1:20 (w/w) at 37°C for 16 hrs. The trypsin digestion products were analysed on 13% SDS polyacrylamide gel.

16.2 Disulphide Bond Determination (78)

Gel-shift assays were employed to indicate the existence of the disulphide bond. The solubilized wild type and mutant protoxins were digested with trypsin as described in **METHOD 16.1**. The trypsin-treated toxins were then mixed with 4x sample buffer either containing or lacking 14.4 mM β-mercaptoethanol. Samples were analysed on 13% SDS polyacrylamide gel.

17. Mosquito Larvicidal Activity Assays

Mosquito bioassays were modified from previously described methods (79) using 2-day-old *Aedes aegypti* larvae, obtained from the mosquito-rearing facility of the Institute of Molecular Biology and Genetics, Mahidol University. The *E. coli* strain JM109 harboring either pMEx-B4A expressing the Cry4A wild type toxin, pC192A or pC199A expressing the mutant toxins was grown in LB broth with 100 μg/ml ampicillin at 37°C. Protein expression was induced with 0.1 mM IPTG for 4 hrs. Cell pellet (20 OD_{600} ~ $2*10^9$ cells) was harvested by centrifugation at 6,000 rpm, 4°C for 10 min, resuspended in 4 ml of distilled water (10^8 cells/200 μl) and diluted to 10^7, 10^6 and 10^5 cells in 200 μl of distilled water. Each assay was performed in a 48-well titration plate (11.3 mm well diameter, Costar, MA, USA) containing 10 larvae in 800 μl of distilled water. Then, 200 μl of *E. coli* cell suspensions (10^5-10^8 cells) was added into each well. The total 300 larvae were used for each cell concentration. The mortality was recorded after 24-hr incubation at room temperature. Modified Reed-Muench Method was used to calculate percent mortality of larvae (80). The calculation method was shown in **Table 1**.

Table 1 Pattern for Calculating Percent Mortality by Reed-Muench Method

Bacterial Dilution (cells/ml)	Mortality Ratio	Average value		Accumulated value		Mortality	
		Died	Survived	Died	Survived	Ratio	Percent
(A)	(B)	(C)	(D)	(E)	(F)	(G)	(H)
10^8	9/10, 10/10, 10/10	9.6	0.4	23.5	0.4	23.5/23.9	98.3
10^7	9/10, 8/10, 8/10	8.3	1.7	13.9	2.1	13.9/16.0	85.0
10^6	4/10, 6/10, 4/10	4.6	5.4	5.6	7.5	5.6/18.7	29.9
10^5	1/10, 1/10, 1/10	1.0	9.0	1.0	14.4	1.0/15.4	6.5

The average value (C and D) was mean of total number of died or survived larva per 10 larvae in each well. The accumulated value of died (E) was calculated from the summation of the average value of died (C) from 10^5 cells to the test step of cells. The accumulated value of survived (F) was calculated from the summation of the average value of survived (D) from 10^8 cells to the test step of cells. The accumulated mortality ratio (G) display the accumulated number of dead larvae (E) over the accumulated total number of larvae (E+F). Percent mortality (H) was equal to the accumulated mortality ratio (G) multiply by 100.

Another assay to test the toxicity is use of inclusion bodies obtained from 4-hr IPTG induced *E. coli* strain JM109 harboring either pMEx-B4A, pC192A or pC199A mutant plasmids grown at 37°C. The assay was performed in a 48-well titration plate (11.3 mm well diameter, Costar, MA, USA) containing 10 larvae in 800 μl of distilled water. Then, 200 μl of distilled water (negative control) and 2 μg of inclusion bodies in

200 µl of distilled water was added into each well. The total 300 larvae were used for each clone. The mortality was recorded after 24-hr incubation at room temperature.

CHAPTER V

RESULTS

1. Construction of Recombinant Plasmids for Expressing the Cry4A Toxin

Many attempts have been made to improve the expression of the Cry4A toxin in *E. coli* by constructing the following recombinant plasmids:

1.1 Construction of pET-Recombinant plasmids

In order to improve the expression of the *cry4A* gene by using the T7 promoter, three types of recombinant plasmids, which are (1) the pET-B4A clone containing the T7 promoter followed by the putative *cry4B* promoter, (2) the pET-4A clone containing only the T7 promoter and (3) the pET-4AUTR(-) clone containing only the T7 promoter and the *cry4B*-5'UTR in which 47 nucleotides was deleted, were constructed.

The recombinant plasmid pET-B4A which contains the 3.8 kb fragment comprising the putative c*ry4B* promoter together with the SD sequence and the *cry4A* structural gene isolated from the recombinant plasmid pBA was constructed (see **Fig. 10**). The DNA fragment was ligated to the *Bam*HI-*Sal*I digested pET24(+) vector according to the method as described in **CHAPTER IV**. The ligation product was then transformed into *E. coli* strain BL21(DE3)pLysS and spread on the LB-kanamycin and chloramphenicol agar plate. Sixteen transformants obtained were screened for the presence of the recombinant plasmid by plasmid extraction as described in

CHAPTER IV and *Hin*dIII digestion. It was found that eleven from sixteen clones showed the expected size of two DNA bands of about 6.6 and 2.2 kb (**Fig. 11**).

To generate the recombinant plasmid pET-4A (**Fig. 12**), the 3.7 kb DNA fragment [from *Eco*RI site (90) to *Sal*I site (3833)] containing the SD sequence and the *cry4A* gene isolated from the recombinant plasmid pBA was ligated to the *Sal*I-*Eco*RI digested pET24(+) vector. The ligation product was transformed into *E. coli* strain BL21(DE3)pLysS. Thirty transformants obtained were screened for the presence of the recombinant plasmid by plasmid extraction and *Xba*I digestion. It was found that three clones showed the expected size of one DNA band of about 8.9 kb (**Fig. 13-15**). Furthermore, *Sma*I, *Sal*I, *Hin*dIII, *Eco*RI and *Ava*I digestions were performed to confirm that three clones are the recombinant plasmid pET-4A (**Fig. 13-15**).

Thirdly, construction was made for the recombinant plasmid pET-4AUTR(-) (**Fig. 16**) in which 47 nucleotides of the *cry4B*-5'UTR was deleted. Sited-directed mutagenesis was employed to delete the nucleotide sequence from the 5'UTR by creating the addition *Bam*HI and *Hin*dIII sites. The mutants were screened by *Hin*dIII digestion and then the mutant plasmid was digested with *Bam*HI to delete the unwanted sequence from the 5'UTR and religated. The ligation product was then transformed into *E. coli* strain BL21(DE3)pLysS. Nine transformants were screened for the presence of the recombinant plasmid by plasmid extraction and *Hin*dIII digestion. It was found that eight clones showed the expected size of two DNA bands of about 6.5 and 2.2 kb (**Fig. 17**).

1.2 Construction of the pMEx-Recombinant Plasmid

Further attempt was made to improve the expression of the *cry4A* gene by using the *tac* promoter. The recombinant plasmid pMEx-B4A harboring the *cry4A* gene under control of the *tac* promoter as well as the *cry4B* regulatory region was constructed (**Fig. 18**).

The 3.8 kb DNA fragment containing the *cry4B* regulatory region and the *cry4A* structural gene was purified from pBA and then ligated to the predigested pMEx8 vector. The ligation product was then transformed into *E. coli* strain JM109 and spread on LB-Amp agar. Seven transformants obtained were screened for the presence of the recombinant plasmid by plasmid extraction and *Hin*dIII digestion. It was found that three clones showed the expected size of two DNA bands of about 5.0 and 2.2 kb (**Fig. 19**).

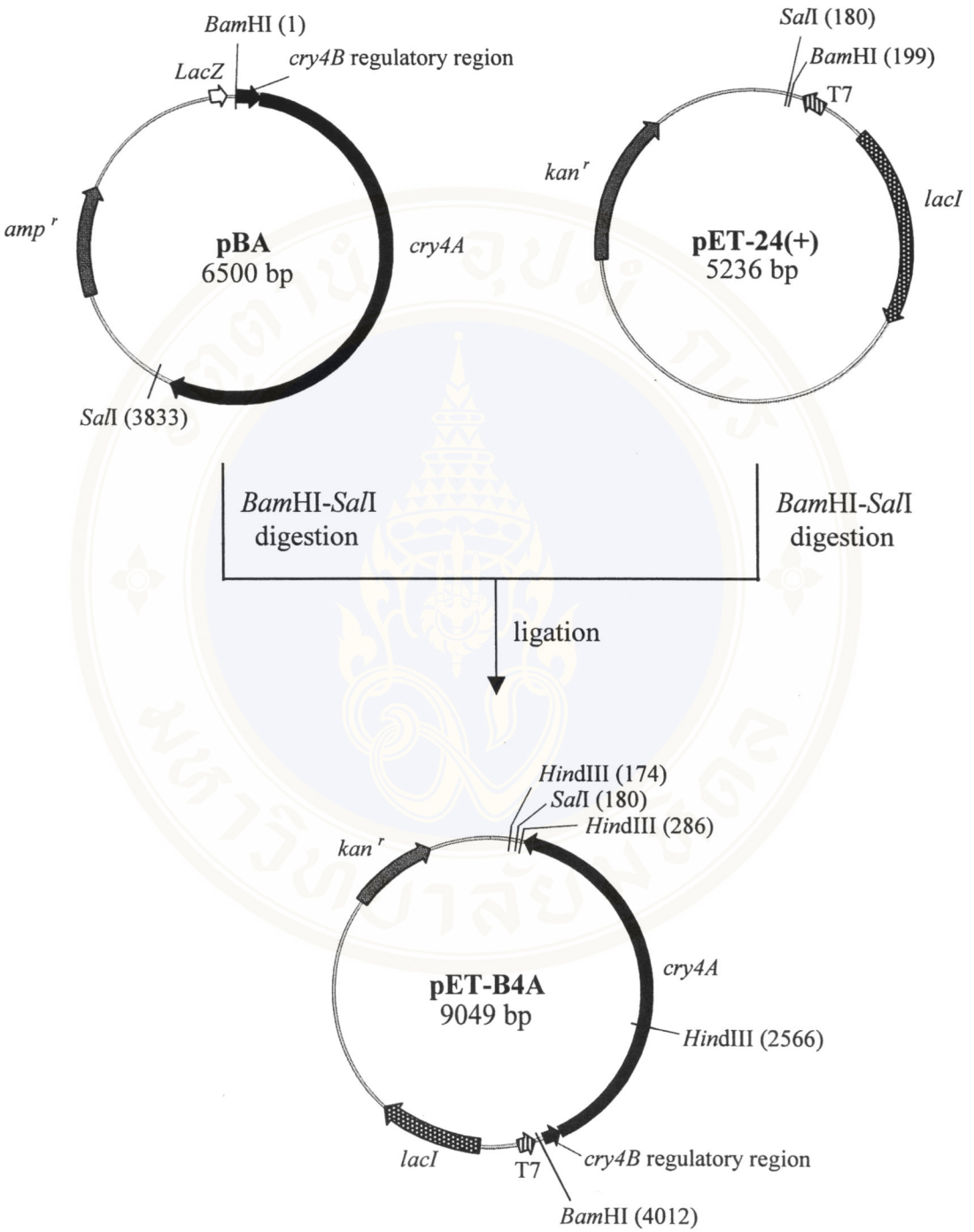

Figure 10 Construction of the recombinant plasmid pET-B4A

The recombinant plasmid pET-B4A was constructed by subcloning the 3.8 kb fragment containing the putative *cry4B* promoter, SD sequence and the *cry4A* gene from pBA into predigested *Bam*HI and *Sal*I sites of the expression vector pET24(+).

Figure 11 Restriction endonuclease analysis of pET-B4A recombinant plasmids
This figure shows 0.8% agarose gel electrophoresis (ethidium bromide stained) of *Hin*dIII digestion pattern of the recombinant plasmids.

Lane 1 : λ / *Hin*dIII digested DNA marker
Lanes 2,4,8-11,13-17 : pET-B4A digested with *Hin*dIII
Lanes 3,5-7,12 : undesirable recombinant plasmids digested with *Hin*dIII

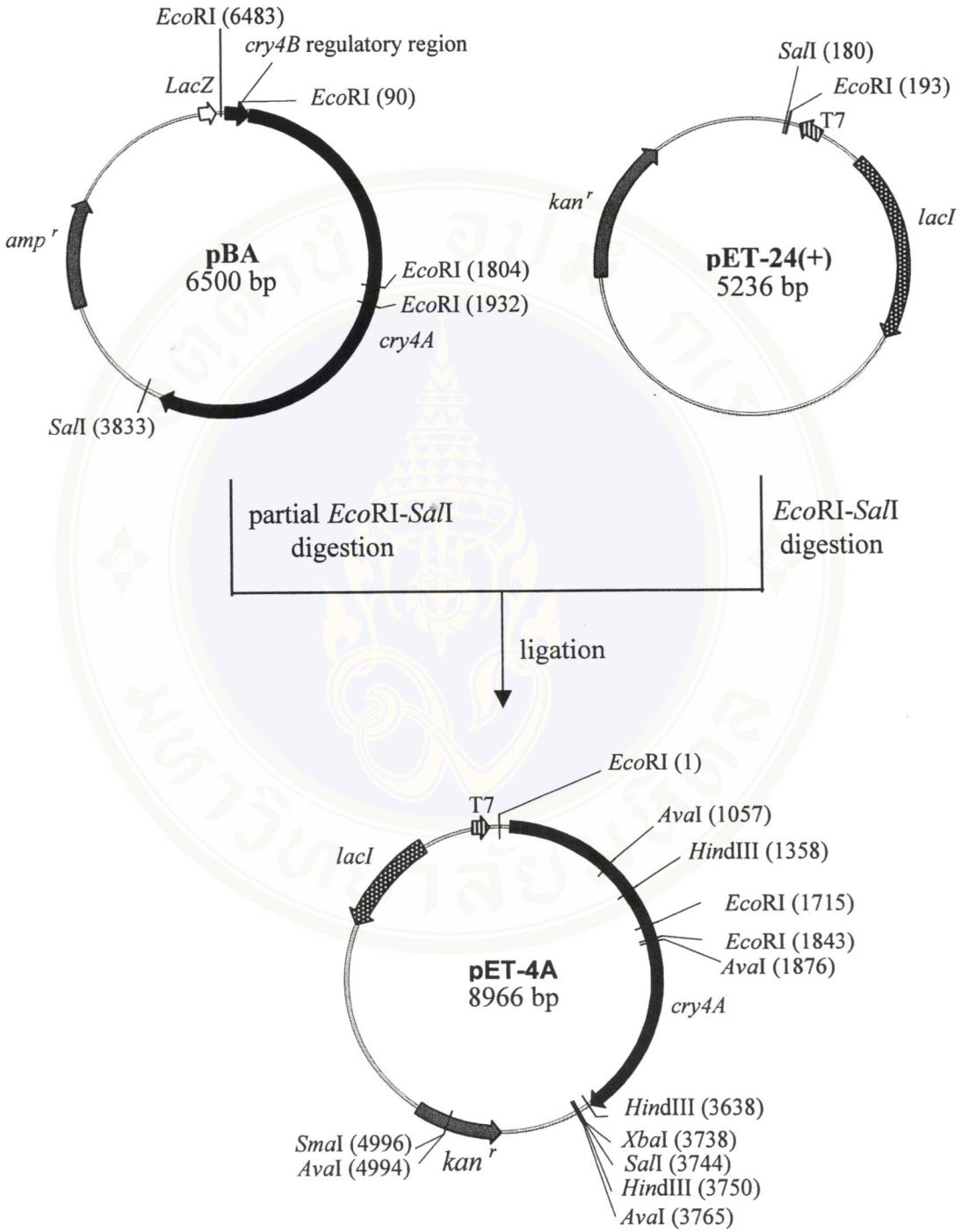

Figure 12 Construction of the recombinant plasmid pET-4A

The recombinant plasmid pET-4A was constructed by subcloning the 3.7 kb fragment containing SD sequence and the *cry4A* gene from pBA into predigested *Eco*RI and *Sal*I sites of the expression vector pET24(+).

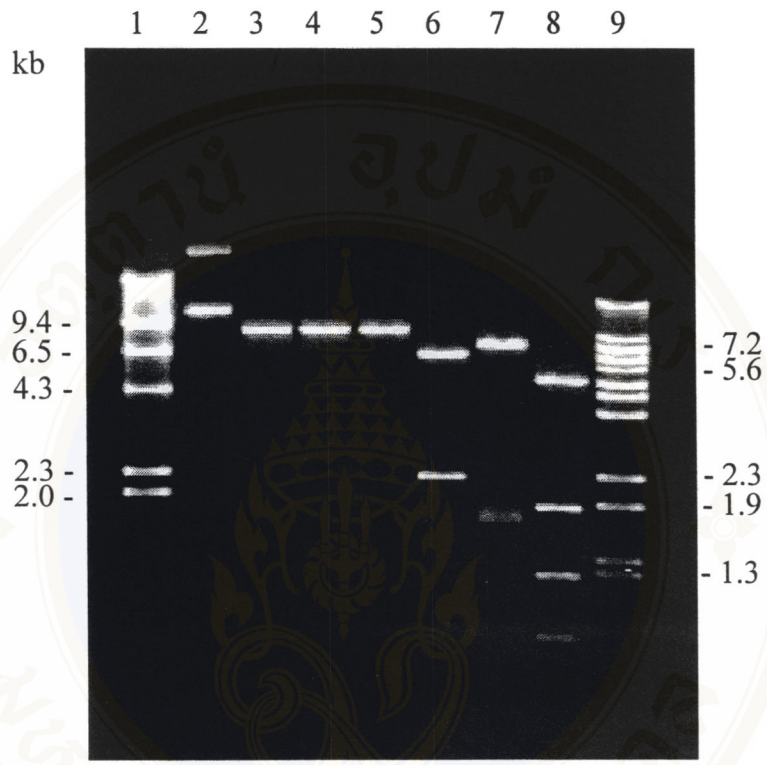

Figure 13 Restriction endonuclease analysis of pET-4A recombinant plasmid

This figure shows 0.8% agarose gel electrophoresis (ethidium bromide stained) of *Xba*I, *Sma*I, *Sal*I, *Hin*dIII, *Eco*RI and *Ava*I digestion patterns of the recombinant plasmid.

Lane 1 : λ / *Hin*dIII digested DNA marker
Lane 2 : the undigested pET-4A
Lane 3 : pET-4A digested with *Xba*I
Lane 4 : pET-4A digested with *Sma*I
Lane 5 : pET-4A digested with *Sal*I
Lane 6 : pET-4A digested with *Hin*dIII
Lane 7 : pET-4A digested with *Eco*RI
Lane 8 : pET-4A digested with *Ava*I
Lane 9 : λ / *Bst*EII digested DNA marker

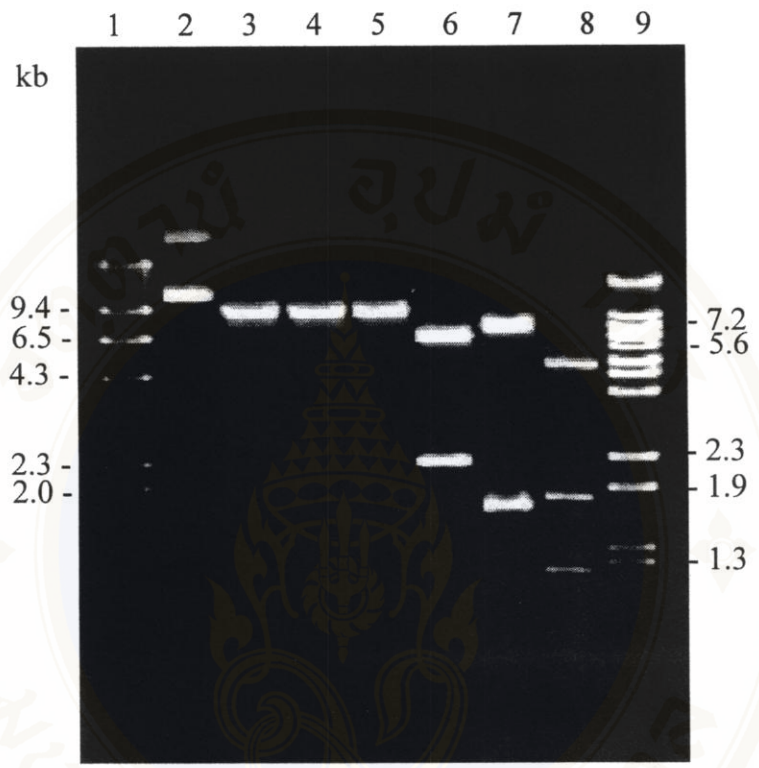

Figure 14 Restriction endonuclease analysis of pET-4A recombinant plasmid

This figure shows 0.8% agarose gel electrophoresis (ethidium bromide stained) of *Xba*I, *Sma*I, *Sal*I, *Hin*dIII, *Eco*RI and *Ava*I digestion patterns of the recombinant plasmid.

Lane 1 : λ / *Hin*dIII digested DNA marker
Lane 2 : the undigested pET-4A
Lane 3 : pET-4A digested with *Xba*I
Lane 4 : pET-4A digested with *Sma*I
Lane 5 : pET-4A digested with *Sal*I
Lane 6 : pET-4A digested with *Hin*dIII
Lane 7 : pET-4A digested with *Eco*RI
Lane 8 : pET-4A digested with *Ava*I
Lane 9 : λ / *Bst*EII digested DNA marker

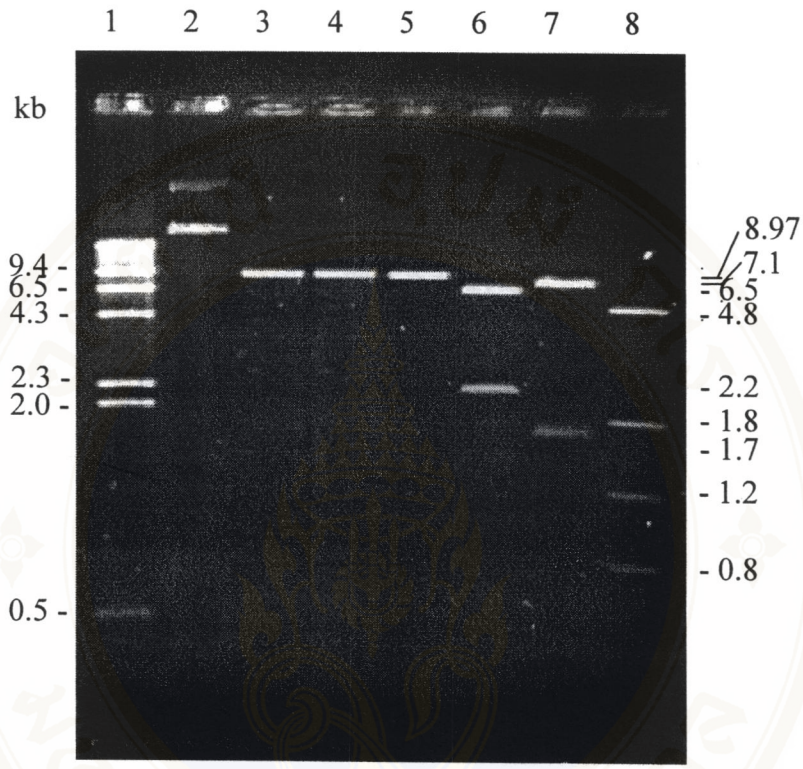

Figure 15 Restriction endonuclease analysis of pET-4A recombinant plasmid

This figure shows 0.8% agarose gel electrophoresis (ethidium bromide stained) of *Xba*I, *Sma*I, *Sal*I, *Hin*dIII, *Eco*RI and *Ava*I digestion patterns of the recombinant plasmid.

Lane 1 : λ / *Hin*dIII digested DNA marker
Lane 2 : the undigested pET-4A
Lane 3 : pET-4A digested with *Xba*I
Lane 4 : pET-4A digested with *Sma*I
Lane 5 : pET-4A digested with *Sal*I
Lane 6 : pET-4A digested with *Hin*dIII
Lane 7 : pET-4A digested with *Eco*RI
Lane 8 : pET-4A digested with *Ava*I

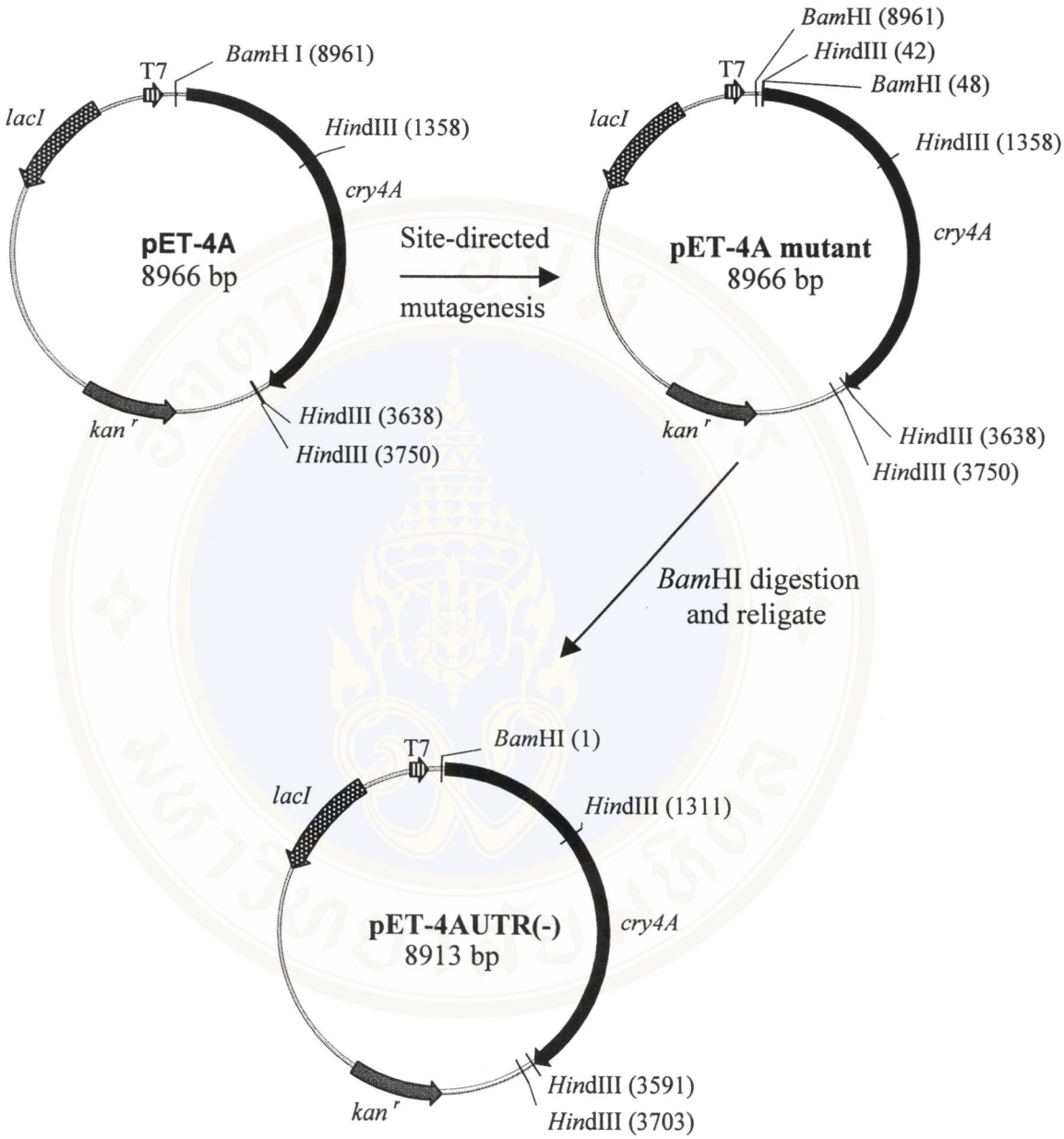

Figure 16 Construction of the recombinant plasmid pET-4AUTR(-)

The figure illustrates the construction of the recombinant plasmid pET-4AUTR(-). Sited-directed mutagenesis was employed to delete the nucleotide sequence from the *cry4B*-5'UTR by creating an addition *Bam*HI site. The mutant plasmid was digested with *Bam*HI to delete 47 nucleotides of the *cry4B*-5'UTR and religated.

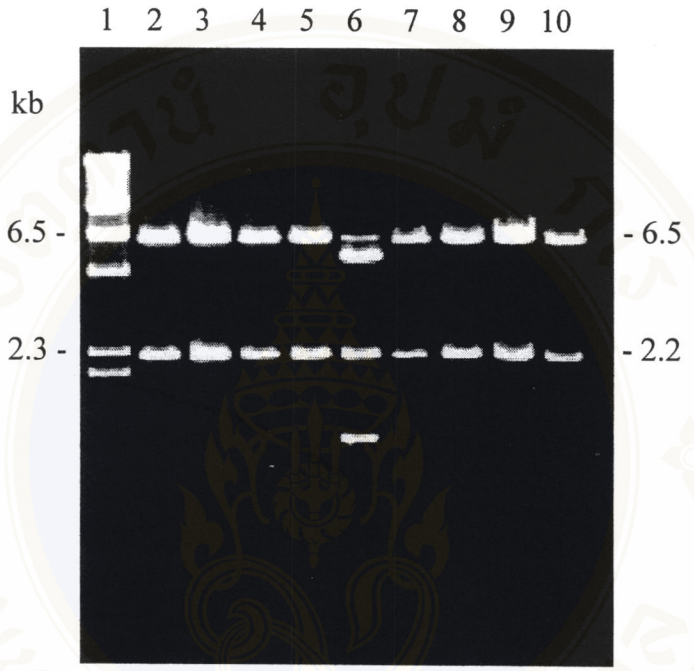

Figure 17 Restriction endonuclease analysis of pET-4AUTR(-) recombinant plasmids

This figure shows 0.8% agarose gel electrophoresis (ethidium bromide stained) of *Hin*dIII digestion pattern of the recombinant plasmids.

Lane 1 : λ / *Hin*dIII digested DNA marker
Lanes 2-5,7-10 : pET-4AUTR(-) digested with *Hin*dIII
Lane 6 : an undesirable recombinant plasmid digested with *Hin*dIII

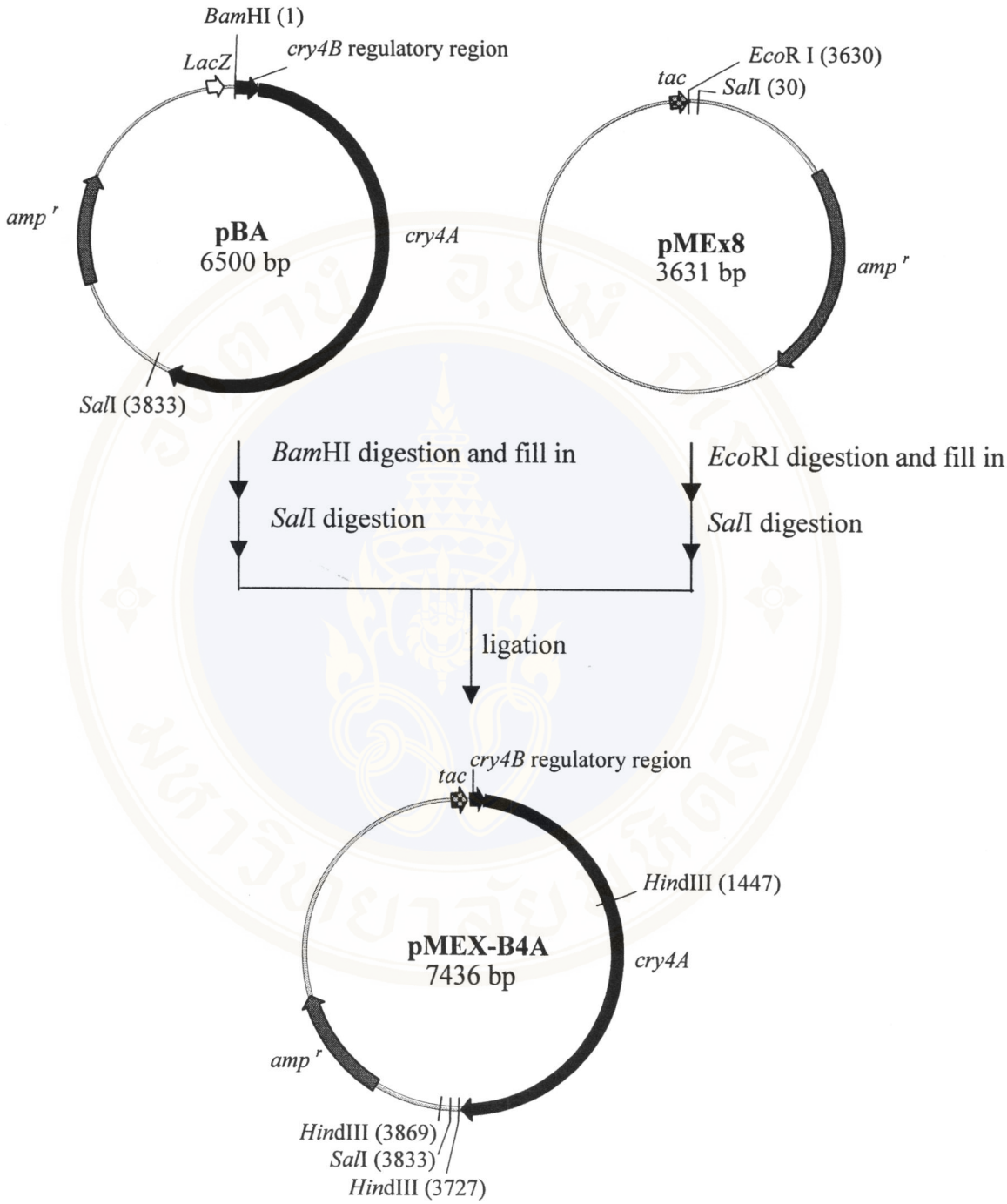

Figure 18 Construction of the recombinant plasmid pMEx-B4A

The recombinant plasmid pMEx-B4A was constructed by subcloning the 3.8 kb fragment containing the putative *cry4B* promoter, SD sequence and the *cry4A* gene from pBA into predigested *Eco*RI and *Sal*I sites of the expression vector pMEx8.

Figure 19 Restriction endonuclease analysis of pMEx-B4A recombinant plasmids
This figure shows 0.8% agarose gel electrophoresis (ethidium bromide stained) of *Hin*dIII digestion pattern of the recombinant plasmids.

Lane 9 : λ / *Bst*EII digested DNA marker
Lanes 1,3,14 : the undigested pMEx-B4A
Lanes 2,4,15 : pMEx-B4A digested with *Hin*dIII
Lanes 5,7,10,12 : the undigested undesirable recombinant plasmids
Lanes 6,8,11,13 : undesirable recombinant plasmids digested with *Hin*dIII

2. Expression of the Wild-Type Cry4A Toxin

All pET-recombinant plasmids were expressed in *E. coli* strain BL21(DE3)pLysS and the recombinant plasmid pBA was expressed in *E. coli* strain JM109 upon induction with IPTG as described in **CHAPTER IV**. When the cells were lysed and subjected to 10% SDS-PAGE, it was found that all three types of the pET-recombinant plasmids expressed the level of the 130 kDa Cry4A toxin lower than the original clone (pBA) containing the *cry4A* gene under control of the *cry4B* regulatory region and the *LacZ* promoter (**Fig. 20**). Interestingly, *E. coli* strain JM109 containing pMEx-B4A exhibited higher expression level of the Cry4A toxin than the pBA clone (**Fig. 21**).

The optimum point for expressing the Cry4A toxin from *E. coli* containing pMEx-B4A was also determined by collecting the bacterial culture at different time of induction. It was found that the Cry4A protein reached the highest level after 4 hrs of induction (**Fig. 21**) and at this time point, the Cry4A toxin was expressed as a cytoplasmic inclusion (**Fig. 22**).

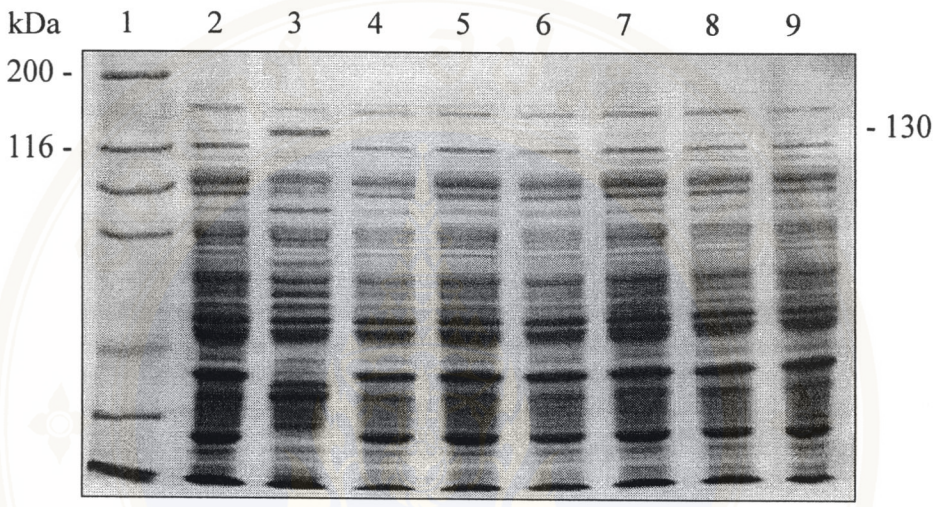

Figure 20 Expression of the Cry4A toxin via the pET vector

The figure shows SDS-PAGE protein profiles (Coomassie blue stained 10% gel) of the crude extracts of IPTG induced *E. coli* recombinant cells containing different plasmids.

Lane 1 : molecular mass protein standards
Lane 2 : crude extracted proteins of *E. coli* containing pET24(+), 4 hrs of induction
Lane 3 : crude extracted proteins of *E. coli* containing pBA, 4 hrs of induction
Lanes 4-5 : crude extracted proteins of *E. coli* containing pET-B4A, 2 and 4 hrs of induction
Lanes 6-7 : crude extracted proteins of *E. coli* containing pET-4A, 2 and 4 hrs of induction
Lanes 8-9 : crude extracted proteins of *E. coli* containing pET4AUTR(-), 2 and 4 hrs of induction

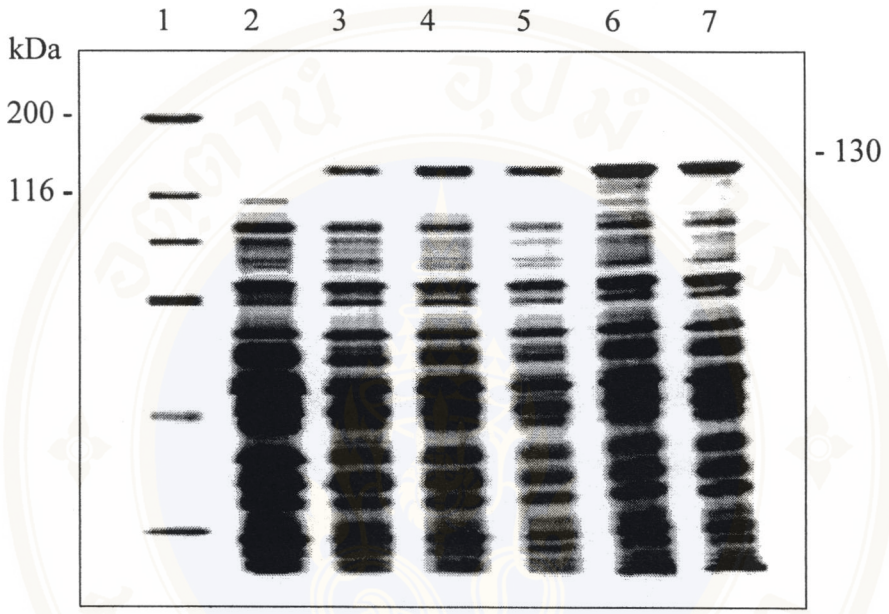

Figure 21 Expression of the Cry4A toxin via the pMEx vector

The figure shows SDS-PAGE protein profiles (Coomassie blue stained 10% gel) of the crude extracts of *E. coli* recombinant cells containing different plasmids expressed at 37°C.

Lane 1 : molecular mass protein standards
Lane 2 : crude extracted proteins of *E. coli* containing pMEx8, 4 hrs of induction
Lane 3 : crude extracted proteins of *E. coli* containing pBA, 4 hrs of induction
Lane 4 : crude extracted proteins of *E. coli* containing pMEx-B4A, non-induced with IPTG grown for 6 hrs
Lanes 5-7 : crude extracted proteins of *E. coli* containing pMEx-B4A, 2,4 and 6 hrs of induction, respectively

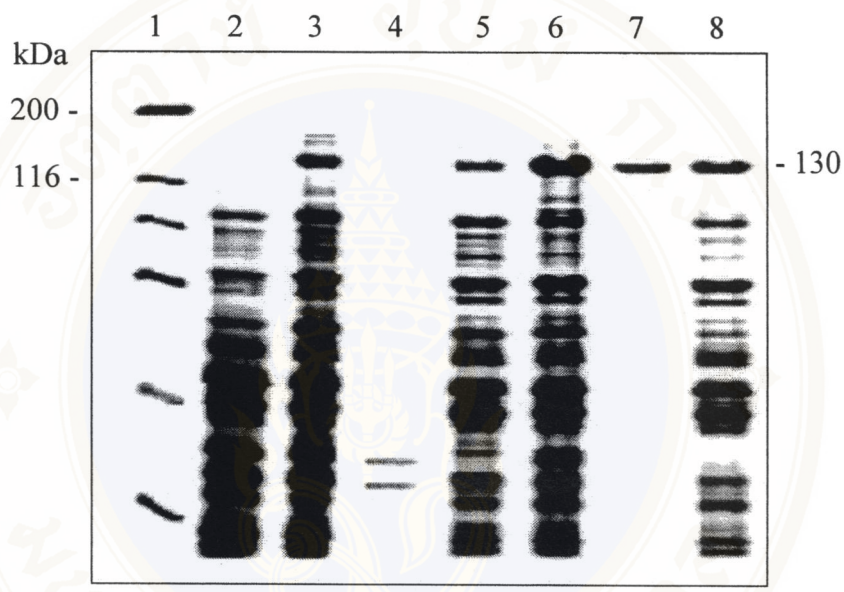

Figure 22 Protein profiles of extracted protein fractions from *E. coli* cells containing either pBA or pMEx-B4A

The figure shows SDS-PAGE protein profiles (Coomassie blue stained 10% gel) of the crude extracts, sedimented protein and supernatant fraction prepared from 4-hr IPTG induced *E. coli* clones grown at 37°C.

Lane 1 : molecular mass protein standards
Lane 2 : crude extracted proteins of *E. coli* containing pMEx8
Lanes 3-5 : crude extracted, sedimented protein and supernatant fraction from *E. coli* containing pBA, respectively
Lanes 6-8 : crude extracted, sedimented protein and supernatant fraction from *E. coli* containing pMEx-B4A, respectively

3. Biochemical Characterization of Wild-type Cry4A Toxin

3.1 Solubility and Proteolytic Activation of Cry4A Toxin

Solubility analysis of the Cry4A inclusions in carbonate buffer, pH 9.0 showed that no soluble protoxin could be recovered for the inclusions obtained from 4-hr IPTG induced *E. coli* clones grown at 37°C (**Fig. 23**). Thus, an attempt was made to solubilize the Cry4A inclusions by using various concentrations of urea as shown in **Fig. 24**. It was found that the inclusions were able to be solubilized in 6 M urea. Since, it is not practicable to *in vitro* refold and unfold the 130-kDa Cry4A toxin which is quite large and comprises of three globular clusters, an attempt has been made to overcome the problem by optimizing the solubility profile which may depend on the time of induction. It was however, found that no soluble protoxin could be recovered for the inclusions obtained from 2, 4 and 6-hr IPTG induced *E. coli* clones, grown at 37°C (**Fig. 25**).

To improve the solubilization of Cry4A inclusions, another approach has been tried to express the protein of interest at 30°C. It was interestingly found that the solubility of the inclusions produced from 10-hr IPTG induced clones grown at 30°C increased substantially (**Fig. 27**), although amounts of the protoxin inclusions obtained were lower than that of the cells grown at 37°C (**Fig. 26**).

For proteolytic activation, the solubilized protoxins were digested with trypsin and subjected to 13% SDS-PAGE. It was found that the Cry4A protein was processed into a 47-kDa polypeptide and a ca. 20 kDa fragment composed of α1-α5, similar to the Cry4B toxin (**Fig. 28**).

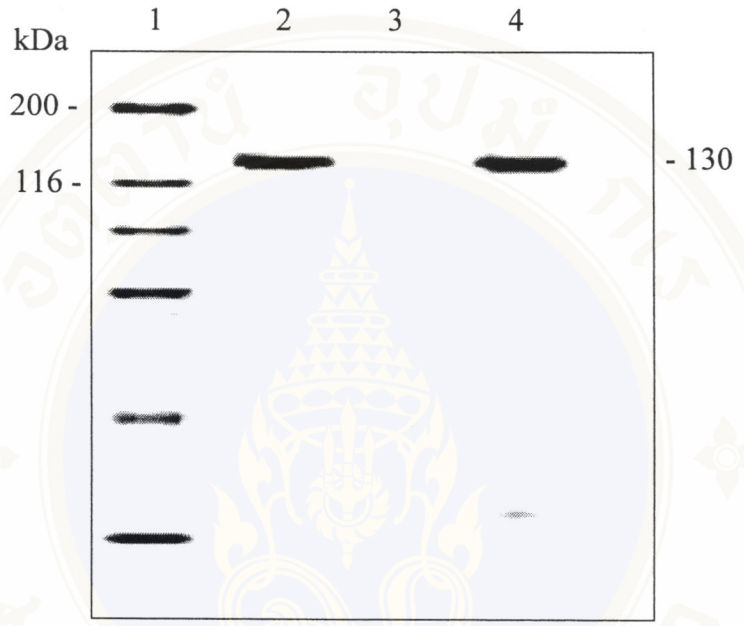

Figure 23 Solubility of the Cry4A toxin inclusions in carbonate buffer

The figure shows SDS-PAGE protein profiles (Coomassie blue stained 10% gel) of the Cry4A inclusions obtained from 4-hr IPTG induced *E. coli* clones grown at 37°C. The toxins were incubated for 1 hr with carbonate buffer (pH 9.0) and centrifuged at 10,000 for 10 min. Prior- and post-centrifugation toxin samples were applied to the gel.

Lane 1 : molecular mass protein standards
Lane 2 : the partially purified Cry4A inclusions
Lane 3 : the solubilized fraction
Lane 4 : the insolubilized Cry4A toxin

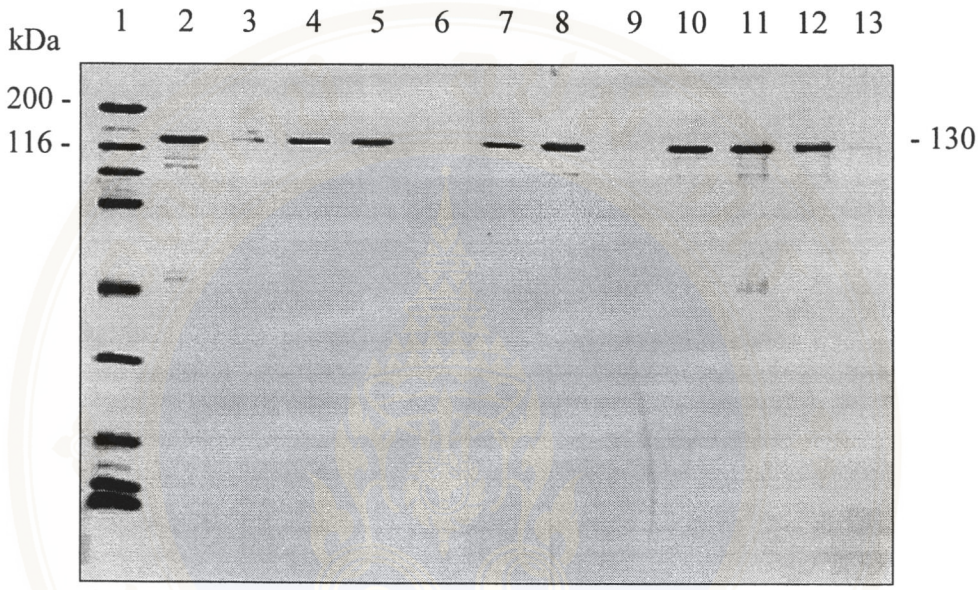

Figure 24 Solubility of the Cry4A toxin inclusions in urea buffer

The figure shows SDS-PAGE protein profiles (Coomassie blue stained 10% gel) of the Cry4A inclusions obtained from 4-hr IPTG induced *E. coli* clones grown at 37°C. The toxins were incubated for 1 hr with various concentrations of urea and centrifuged at 10,000 for 10 min. Prior- and post-centrifugation toxin samples were applied to the gel.

Lane 1 : molecular mass protein standards
Lanes 2-4 : the partially purified inclusion, the solubilized fraction and the insolubilized Cry4A toxin, respectively : 0.5 M urea
Lanes 5-7 : the partially purified inclusion, the solubilized fraction and the insolubilized Cry4A toxin, respectively : 1 M urea
Lanes 8-10 : the partially purified inclusion, the solubilized fraction and the insolubilized Cry4A toxin, respectively : 3 M urea
Lanes 11-13 : the partially purified inclusion, the solubilized fraction and the insolubilized Cry4A toxin, respectively : 6 M urea

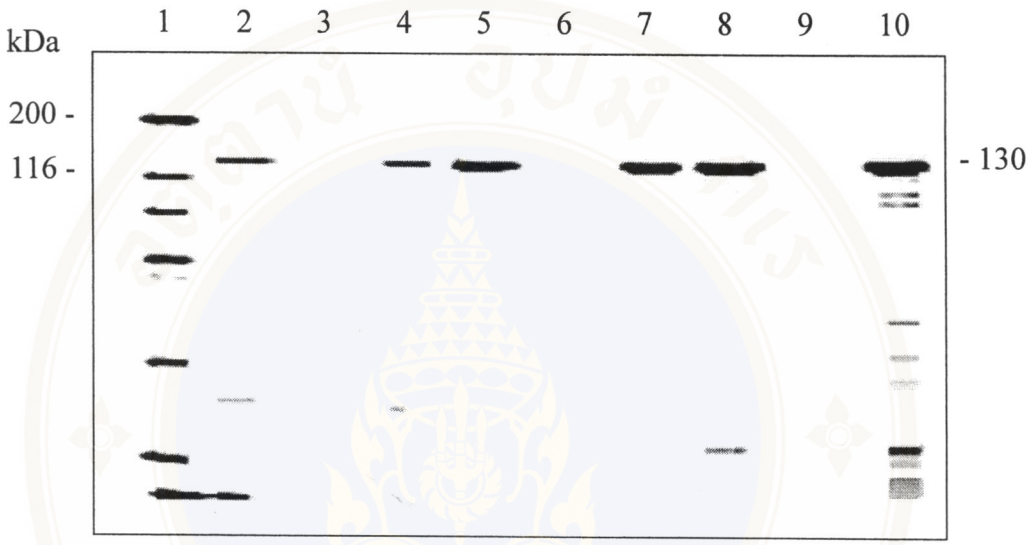

Figure 25 Solubility of the Cry4A toxin inclusions prepared from clones grown at 37°C

The figure shows SDS-PAGE protein profiles (Coomassie blue stained 10% gel) of the Cry4A inclusions obtained from IPTG induced *E.coli* clones grown at 37°C, different time of induction. The toxins were incubated for 1 hr with carbonate buffer (pH 9.0) and centrifuged at 10,000 for 10 min. Prior- and post-centrifugation toxin samples were applied to the gel.

Lane 1 : molecular mass protein standards
Lanes 2-4 : the partially purified inclusion, the solubilized fraction and the insolubilized Cry4A toxin, respectively : 2 hrs of induction
Lanes 5-7 : the partially purified inclusion, the solubilized fraction and the insolubilized Cry4A toxin, respectively : 4 hrs of induction
Lanes 8-10 : the partially purified inclusion, the solubilized fraction and the insolubilized Cry4A toxin, respectively : 6 hrs of induction

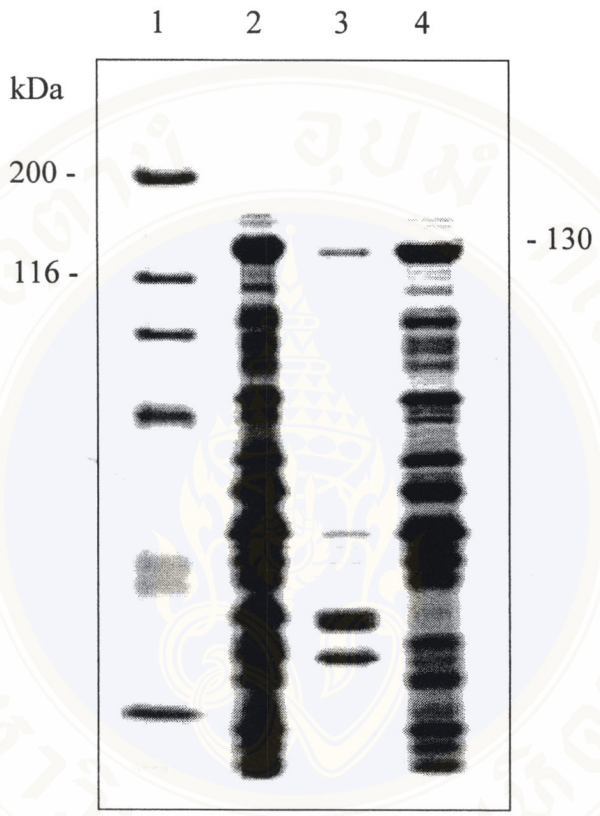

Figure 26 Protein profiles of extracted protein fractions from *E. coli* cells containing pMEx-B4A

The figure shows SDS-PAGE protein profiles (Coomassie blue stained 10% gel) of the crude extracts, sedimented protein and supernatant fraction prepared from 10-hr IPTG induced *E. coli* clones grown at 30°C.

Lane 1 : molecular mass protein standards
Lane 2-4 : crude extracted, sedimented protein and supernatant fraction from *E. coli* containing pMEx-B4A

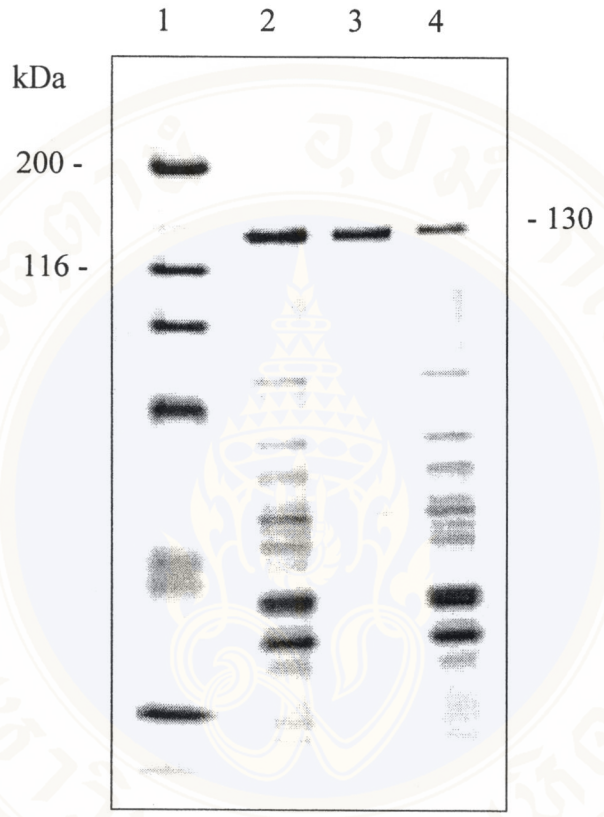

Figure 27 Solubility of the Cry4A toxin inclusions prepared from clones grown at 30°C

The figure shows SDS-PAGE protein profiles (Coomassie blue stained 10% gel) of the Cry4A inclusions obtained from 10-hr IPTG induced *E. coli* clones grown at 30°C. The toxins were incubated for 1 hr with carbonate buffer (pH 9.0) and centrifuged at 10,000 for 10 min. Prior- and post-centrifugation toxin samples were applied to the gel.

Lane 1 : molecular mass protein standards
Lane 2 : the partially purified Cry4A inclusions
Lane 3 : the solubilized fraction
Lane 4 : the insolubilized Cry4A toxin

3.2 Disulphide Bond Determination

To determine the existence of the disulphide bond, gel-shift assays were employed. Based on the fact that, the protein containing the disulphide bonds will have mobility faster than the one lacking the disulphide bond under non-reducing conditions. When the activated wild type toxins were analysed on SDS-PAGE, it was found that the 20-kDa fragment of the wild type protein treated with β-mercaptoethanol had mobility slower than the untreated protein (**Fig. 28, lanes 2-3**), suggesting the existence of the C192-C199 disulphide bond within the loop connecting α4 and α5 of the Cry4A toxin.

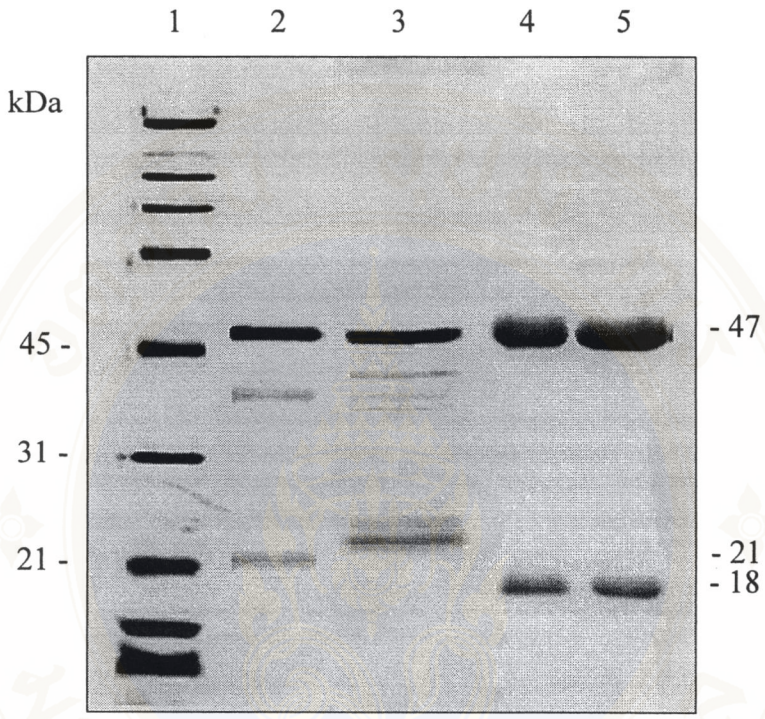

Figure 28 Trypsin digestion products of the Cry4A and Cry4B toxins

The figure shows SDS-PAGE protein profiles (Coomassie blue stained 13% gel) of the trypsin digestion products of the Cry4A and Cry4B toxins.

Lane 1 : molecular mass protein standards
Lane 2 : the trypsin digestion products of the Cry4A toxin untreated with β-mercaptoethanol
Lane 3 : the trypsin digestion products of the Cry4A toxin treated with β-mercaptoethanol
Lane 4 : the trypsin digestion products of the Cry4B toxin untreated with β-mercaptoethanol
Lane 5 : the trypsin digestion products of the Cry4B toxin treated with β-mercaptoethanol

4. Construction of the Non-Disulphide Bridged Mutants

For construction of the two non-disulphide bridged mutant plasmids, pC192A and pC199A were generated via site-directed mutagenesis. The recombinant plasmid pMEx-B4A (**Fig. 18**) containing the gene sequence encoding the 130-kDa Cry4A toxin was used as a template together with the two mutagenesis primers which were designed to substitute the mutated bases and introduced a restriction enzyme recognition site for screening the mutant plasmid. The *Pfu* DNA Polymerase was employed to achieve highest fidelity. After amplification reaction, the amplified products were analysed on 0.8% agarose gel electrophoresis. It was found that the PCR products showed the expected sizes of DNA band of about 7.4 kb (**Fig. 29** and **Fig. 30**).

After digesting the methylated and hemimethylated plasmid DNA with *Dpn*I, the digested PCR products were transformed into *E.coli* strain JM109. Nine transformants were screened for the presence of the mutant plasmid pC192A via *Eco*RI digestion. It was found that six clones showed the expected size of three DNA bands of about 5.6, 1.1 and 0.6 kb (**Fig. 31**). Eighteen transformants were screened for the presence of the mutant plasmid pC199A via *Ava*I digestion. Seven clones contained the expected size of three DNA bands of about 6.2, 0.8 and 0.4 kb (**Fig. 32**).

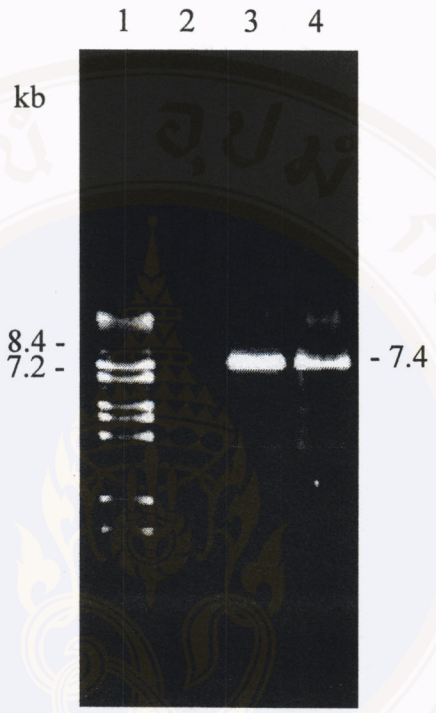

Figure 29 Amplification of the mutant plasmid pC192A

This figure shows 0.8% agarose gel electrophoresis (ethidium bromide stained) of PCR product, using C192A-f and C192A-r as primers, pMEx-B4A as template and 48°C as annealing temperature.

Lane 1 : λ / *Bst*EII digested DNA marker
Lane 2 : negative control using sterile distilled water instead of DNA template in the reaction
Lane 3 : the PCR product of the mutant plasmid pC192A
Lane 4 : the PCR product of the mutant plasmid pC192A digested with *Dpn*I

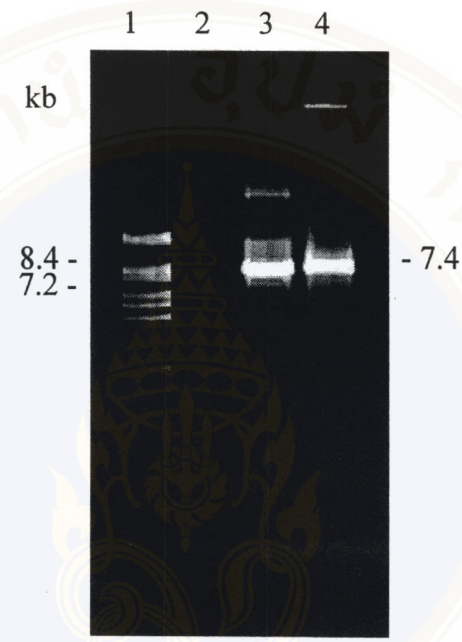

Figure 30 Amplification of the mutant plasmid pC199A

This figure shows 0.8% agarose gel electrophoresis (ethidium bromide stained) of PCR product, using C199A-f and C199A-r as primers, pMEx-B4A as template and 45°C as annealing temperature.

Lane 1 : λ / *Bst*EII digested DNA marker
Lane 2 : negative control using sterile distilled water instead of DNA template in the reaction
Lane 3 : the PCR product of the mutant plasmid pC199A
Lane 4 : the PCR product of the mutant plasmid pC199A digested with *Dpn*I

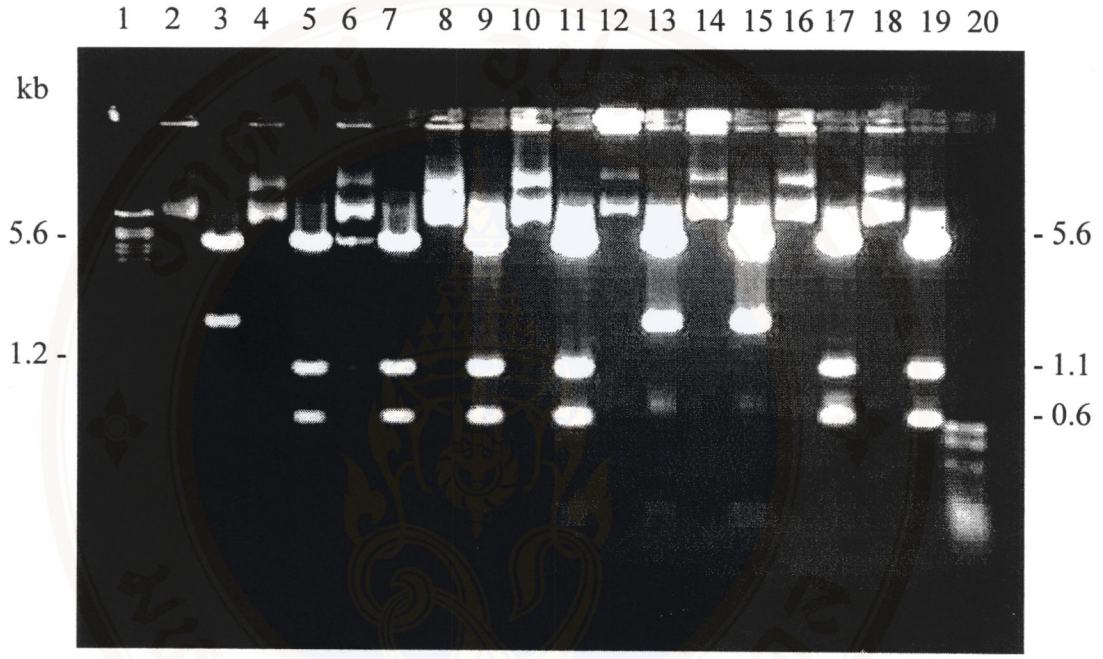

Figure 31 Restriction endonuclease analysis of pC192A mutant plasmids

This figure shows 1.0% agarose gel electrophoresis (ethidium bromide stained) of *Eco*RI digestion pattern of the mutant plasmids.

Lane 1	: λ / *Bst*EII digested DNA marker
Lanes 4,6,8,10,16,18	: the undigested pC192A
Lanes 5,7,9,11,17,19	: pC192A digested with *Eco*RI
Lanes 2,12,14	: the undigested undesirable mutant plasmid
Lanes 3,13,15	: undesirable mutant plasmid digested with *Eco*RI
Lane 20	: pBR322/*Msp*I digested DNA marker

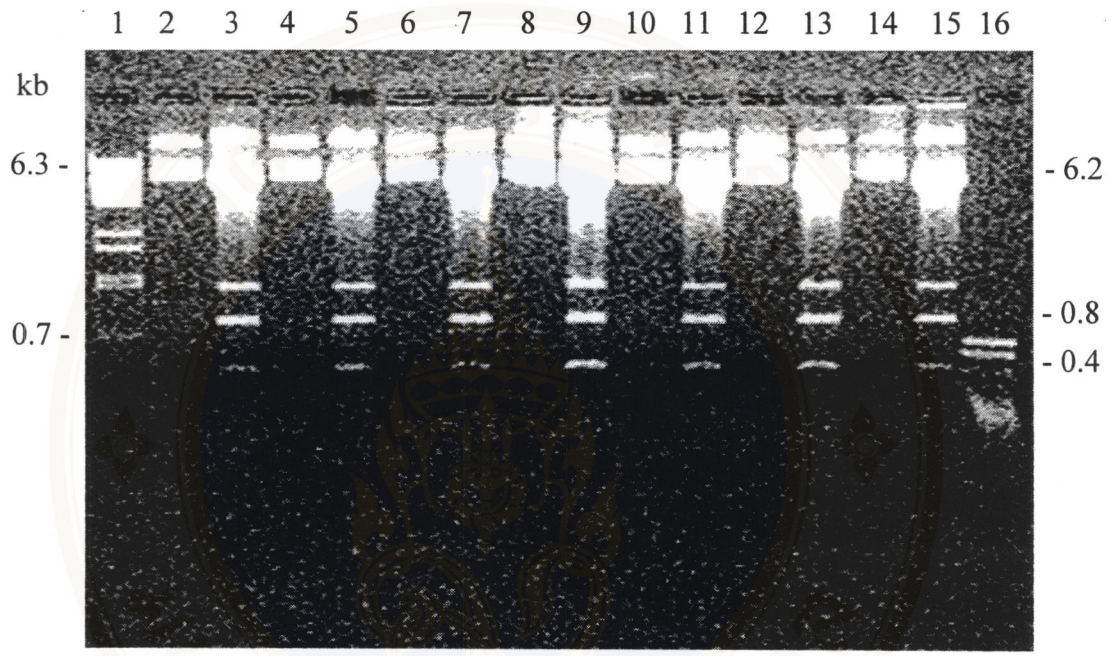

Figure 32 Restriction endonuclease analysis of pC199A mutant plasmids

This figure shows 1.0% agarose gel electrophoresis (ethidium bromide stained) of *Ava*I digestion pattern of the mutant plasmids.

Lane 1 : λ / *Bst*EII digested DNA marker
Lanes 2,4,6,8,10,12,14 : the undigested pC199A
Lanes 3,5,7,9,11,13,15 : pC199A digested with *Ava*I
Lane 16 : pBR322/*Msp*I digested DNA marker

5. Expression of the Non-Disulphide Bridged Mutants

The mutant plasmids were expressed in *E.coli* strain JM109 upon induction with IPTG as described in **CHAPTER IV**. When the cells were lysed and subjected to 10% SDS polyacrylamide gel, it was found that clone 4 of both pC192A and pC199A exhibited high expression of the 130-kDa protein (**Fig. 33**), so these two clones were chosen to express the mutant toxins for further analysis.

Like the wild-type Cry4A protein, the non-disulphide bridged mutants were expressed in both soluble and inclusion forms at 30°C, 10 hrs of induction (**Fig. 34**).

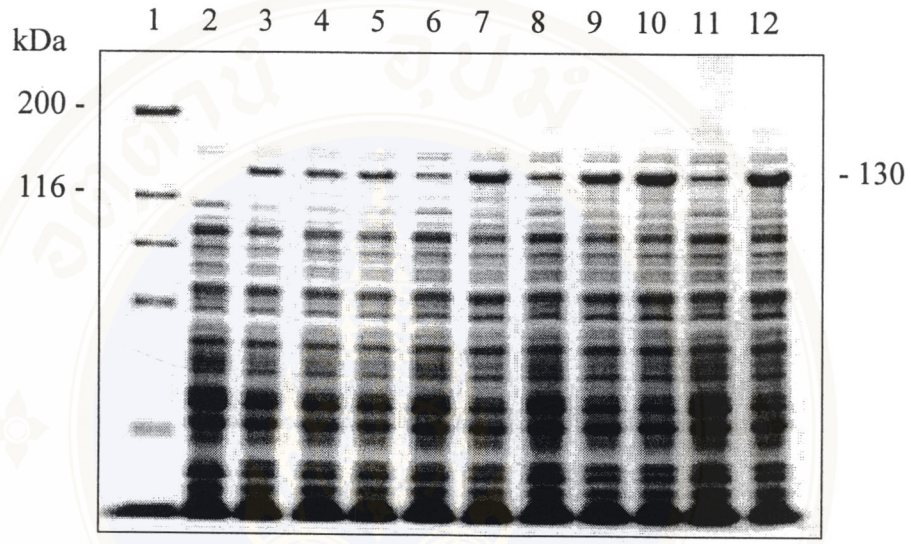

Figure 33 Expression level of the wild type and mutant Cry4A toxins

The figure shows SDS-PAGE protein profiles (Coomassie blue stained 10% gel) of the crude extracts of 4-hr IPTG induced *E. coli* recombinant cells containing either pMEx-B4A, pC192A or pC199A expressed at 37°C.

Lane 1 : molecular mass protein standards
Lane 2 : crude extracted proteins of *E. coli* containing pMEx8
Lane 3 : crude extracted proteins of *E. coli* containing pMEx-B4A
Lanes 4-8 : crude extracted proteins of *E. coli* containing pC192A clones 1-5, respectively
Lanes 9-12 : crude extracted proteins of *E. coli* containing pC199A clones 1-4, respectively

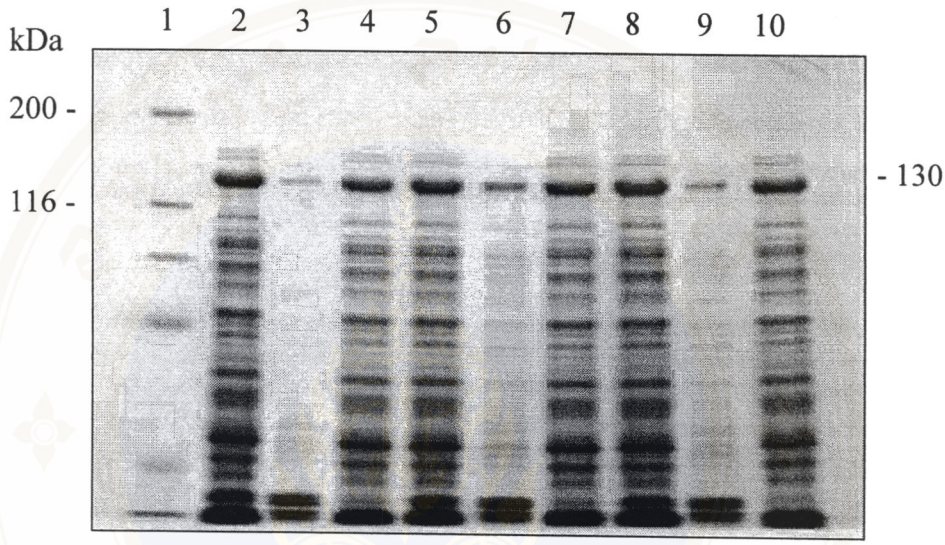

Figure 34 Protein profiles of extracted protein fractions from *E. coli* cells containing either pMEx-B4A, pC192A or pC199A

The figure shows SDS-PAGE protein profiles (Coomassie blue stained 10% gel) of the crude extracts, sedimented protein and supernatant fraction prepared from 10-hr IPTG induced *E. coli* clones grown at 30°C.

Lane 1 : molecular mass protein standards
Lanes 2-4 : crude extracted, sedimented protein and supernatant fraction from *E. coli* containing pMEx-B4A
Lanes 5-7 : crude extracted, sedimented protein and supernatant fraction from *E. coli* containing pC192A
Lanes 8-10 : crude extracted, sedimented protein and supernatant fraction from *E. coli* containing pC199A

6. Biochemical Characterization of the Mutant Cry4A Toxins

6.1 Solubility and Proteolytic Activation of Mutant Cry4A Toxins

Similar to the wild type Cry4A protein, the mutant Cry4A inclusions produced from 10-hr IPTG induced *E. coli* clones grown at 30°C were able to be solubilized in carbonate buffer, pH 9.0 (**Fig. 35**).

After solubilization and trypsin digestion, both mutant Cry4A proteins were processed into a 47-kDa polypeptide and a ca. 20-kDa fragment composed of α1- α5 (**Fig. 36**). The fact that the stably expressed mutants exhibited the same solubility characteristics as the wild type protoxin and generated stable products when treated with trypsin suggested that they had folded correctly.

6.2 Disulphide Bond Determination

Gel-shift assays were performed to confirm disappearance of the pre-existent disulphide bond. When the activated wild type and mutant toxins were analysed on SDS-PAGE, it was found that the 20-kDa fragment of the wild type protein treated with β-mercaptoethanol had mobility slower than the untreated protein **(Fig. 36, lanes 2-3)** while that of both mutant proteins when treated with β-mercaptoethanol had the same mobility as the untreated proteins (**Fig. 36, lanes 4-7**), suggesting the disappearance of the C192-C199 disulphide bond within the interhelical loop.

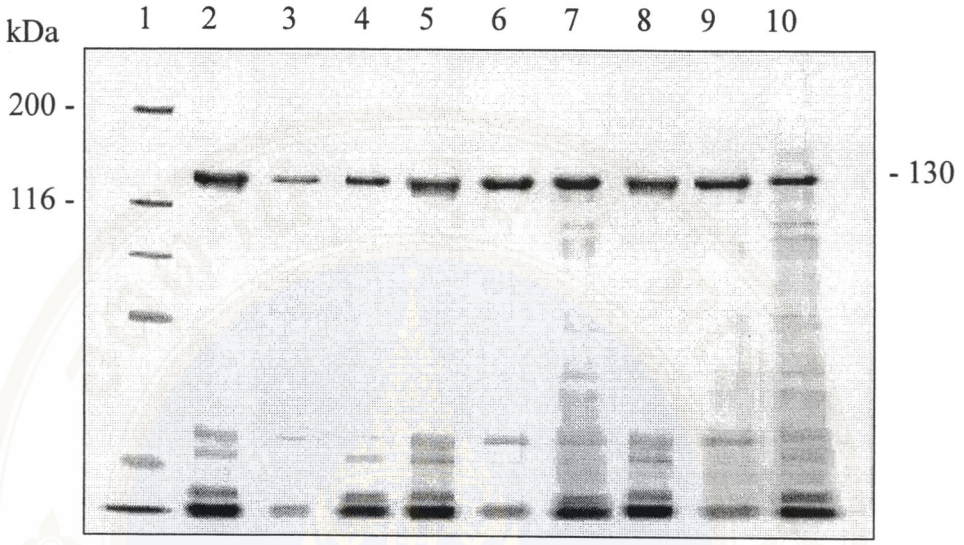

Figure 35 Solubility of the wild type and mutant Cry4A toxin inclusions

The figure shows SDS-PAGE protein profiles (Coomassie blue stained 10% gel) of the wild type and mutant Cry4A inclusions obtained from 10-hr IPTG induced *E. coli* clones grown at 30°C. The toxins were incubated for 1 hr with carbonate buffer (pH 9.0) and centrifuged at 10,000 for 10 min. Prior- and post-centrifugation toxin samples were applied to the gel.

Lane 1 : molecular mass protein standards
Lane 2 : the partially purified wild type Cry4A inclusions
Lane 3 : the solubilized wild type Cry4A toxin
Lane 4 : the insolubilized wild type Cry4A toxin
Lane 5 : the partially purified C192A mutant inclusions
Lane 6 : the solubilized C192A mutant toxin
Lane 7 : the insolubilized C192A mutant toxin
Lane 8 : the partially purified C199A mutant inclusions
Lane 9 : the solubilized C199A mutant toxin
Lane 10 : the insolubilized C199A mutant toxin

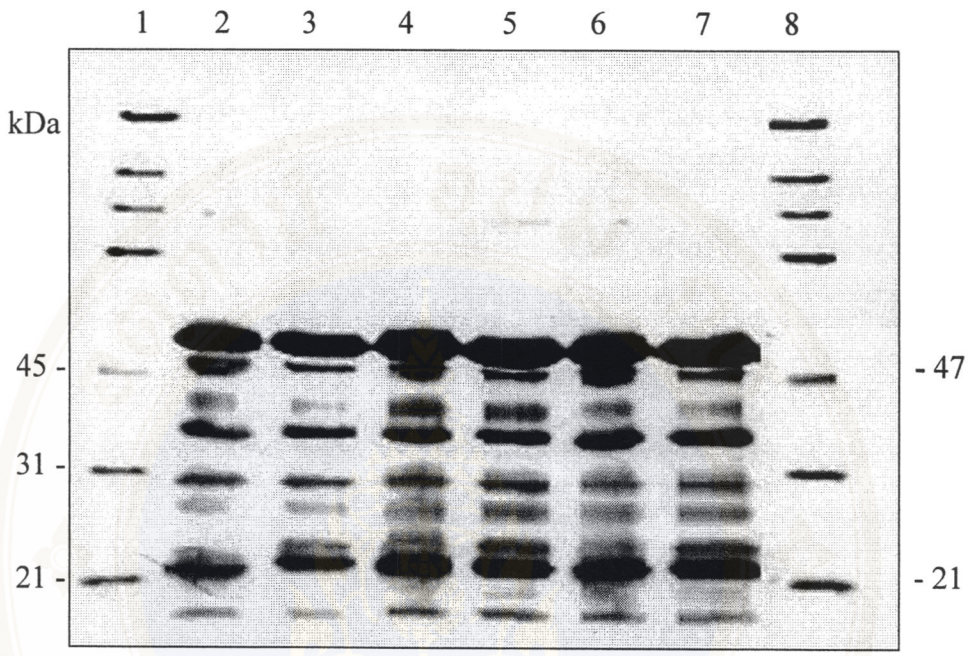

Figure 36 Trypsin digestion products of the wild type and mutant Cry4A toxins

The figure shows SDS-PAGE protein profiles (Coomassie blue stained 13% gel) of the trypsin digestion products of the wild type, C192A and C199A mutant Cry4A toxins.

Lanes 1,8 : molecular mass protein standards.
Lanes 2,4,6 : the trypsin digestion products of the wild type, C192A and C199A mutant Cry4A toxins untreated with β-mercaptoethanol, respectively
Lanes 3,5,7 : the trypsin digestion products of the wild type, C192A and C199A mutant Cry4A toxins treated with β-mercaptoethanol, respectively

7. Mosquito Larvicidal Activity Assays

Mosquito bioassays were performed with either *E. coli* whole cells or inclusion bodies produced from 4-hr IPTG induced *E. coli* clones harboring either pMEx-B4A expressing the Cry4A wild type toxin, pC192A or pC199A expressing the mutant toxins grown at 37°C. These assays were performed to compare the larvicidal activity against 2-day-old *A. aegypti* larvae of the wild type and mutant toxins. Percentage mortality of the larvae after 24-hr exposure to different concentrations of whole cells or inclusions from *E. coli* clones expressing either the Cry4A wild type, C192A or C199A mutant toxins were shown in **Table 2** and **Table 3**, respectively. It was found that *E. coli* cells expressing either mutant in which the pre-existent disulphide bond within the α4-α5 loop was abolished, exhibited approximately the same level of larvicidal activity as the wild type at three different cell concentrations (10^8-10^6 cells/ml). Interestingly, the wild type toxin inclusions (2 μg/ml) were apparently at least 2-fold more toxic than both mutant inclusions.

Table 2 Larvicidal activity of *E. coli* clones expressing either the Cry4A wild type, C192A or C199A mutant toxins

The table shows the larvicidal activities against 2-day-old *A. aegypti* mosquito larvae after 24-hr exposure to different concentrations of *E. coli* cells expressing either the Cry4A wild type, C192A or C199A mutant toxins. The data represent the mean ± SEM based on three separated assays.

E. coli clone containing plasmids	Bacterial Dilution (cells/ml)	% Mortality ± SEM[a]
pMEx-B4A	10^8	97.3 ± 0.2
	10^7	50.9 ± 5.1
	10^6	37.7 ± 4.8
	10^5	25.4 ± 0.9
pC192A	10^8	96.4 ± 0.4
	10^7	46.6 ± 8.0
	10^6	22.8 ± 6.5
	10^5	10.0 ± 1.7
pC199A	10^8	96.1 ± 0.8
	10^7	49.3 ± 5.1
	10^6	22.7 ± 5.5
	10^5	9.3 ± 2.0

[a] SEM = $\frac{SD}{\sqrt{N}}$; [N = Sample size (3)]

Table 3 Larvicidal activity of the inclusions obtained from *E. coli* clones containing either pMEx-B4A, pC192A or pC199A mutant plasmids

The table shows the larvicidal activities against 2-day-old *A. aegypti* mosquito larvae after 24-hr exposure to inclusions obtained from 4-hr IPTG induced *E. coli* clones grown at 37°C expressing either the Cry4A wild type, C192A or C199A mutant toxins. The data represent the mean ± SEM based on three separated assays.

Inclusion (2μg/ml)	% Mortality ± SEM[a]
Negative control	1.7 ± 0.7
pMEx-B4A	28.3 ± 3.4
pC192A	11.0 ± 3.6
pC199A	9.67 ± 3.18

[a] $SEM = \frac{SD}{\sqrt{N}}$; [N = Sample size (3)]

CHAPTER VI

DISCUSSION

Recently, a plausible three-dimensional model for the activated 65-kDa Cry4A δ-endotoxin has been constructed via homology modelling based on the X-ray crystal structure of Cry1Aa. Structural analysis of the model has revealed a putative disulphide bond (C192-C199) within the loop connecting α4 and α5 (40) that may be involved in membrane insertion of helical hairpin α4-α5 of Cry4A. In this study, attempts have been made to investigate the role in toxicity of this disulphide bond within the interhelical loop.

From the previous work (70), the amount of the expressed Cry4A toxin in *E. coli* strain JM109 under control of the *LacZ* promoter as well as the *cry4B* regulatory region from the recombinant plasmid pBA was still not high enough to form an inclusion body. The initial task of this project was therefore to improve the expression of the Cry4A toxin gene in *E. coli* by using a stronger promoter such as the T7 promoter that would lead to inclusion formation. Three types of recombinant plasmids were constructed and expressed in *E.coli* strain BL21(DE3)pLysS upon induction with IPTG. It was found that the pET-B4A clone containing the T7 promoter followed by the putative *cry4B* promoter expressed the level of the Cry4A toxin lower than pBA clone containing the gene under control of the *LacZ* promoter together with the *cry4B* regulatory region. One possible reason is that T7 RNA polymerase has a higher transcription rate than *E.coli* RNA polymerase. Since the putative *cry4B*

promoter which could be utilized by *E.coli* RNA polymerase, is downstream of the T7 regulon, it was possible that T7 RNA polymerase might be obstructed by the preceeding *E.coli* RNA polymerase. However, screening for the better expression of some other recombinant clones should have been carried out. Recombinant plasmid (pET-4A) without the putative *cry4B* promoter was also constructed. It was found that the pET-4A clone which contained only the T7 promoter also exhibited lower expression of the Cry4A toxin than the pBA clone. This may be possibly due to the length of 5'UTR between operator and SD sequence in pET-4A clone is so long (66 nucleotides) and contains the inverted sequences that could allow the operator to form a stem-loop structure that would prevent the 30s ribosomal subunit to bind to the SD sequence. Therefore, an attempt was also made to test this hypothesis by constructing another recombinant plasmid (pET-4AUTR(-)) whose 47 nucleotides of *cry4B*-5'UTR was deleted. This would prevent the operator to form the stem-loop structure. It was also found that the pET-4AUTR(-) clone could not improve the expression of the Cry4A toxin. All of these results suggested that the T7 promoter might not be an appropriate promoter to drive the expression of the *cry4A* gene.

Further attempt was made to improve the expression of the Cry4A toxin gene by using the *tac* promoter. The recombinant plasmid pMEx-B4A harboring the *cry4A* gene under control of the *tac* promoter as well as the *cry4B* regulatory region was constructed. When *E. coli* clone containing pMEx-B4A was induced with IPTG, it produced high amounts of the Cry4A protein which lead to inclusion formation and exhibited higher expression level of the Cry4A toxin than the original clone (pBA) containing the *cry4A* gene under control of the *cry4B* regulatory region and the *LacZ*

promoter. This might be due to the strength of the *tac* promoter together with the *cry4B* regulatory region. However, a role in gene expression of the *cry4B*-5'UTR is needed to be further investigated.

Unlike the inclusions of Cry4B which are soluble in carbonate buffer, pH 9.0, the Cry4A protoxin inclusions obtained from 4-hr IPTG induced *E. coli* clones grown at 37°C were readily soluble only when this buffer was supplemented with 6 M urea. This result imply that the interactions among the molecules are likely to be hydrophobic interactions instead of the normal salt bridge. Eventhough the inclusions were able to be unfolded in 6 M urea, but it is not practicable to *in vitro* refold the 130-kDa Cry4A toxin which is quite large and comprises of three globular clusters. Thus, another try-out was made by optimizing the solubility profile which may depend on the time of induction, but it was shown to be unsuccessful.

Another approach has been tried to express the target protein at 30°C which was reported to be successful (81). It was found that the solubility of inclusions obtained from 10-hr induced clones grown at 30°C increased substantially. This significant improvement in solubility might be due to the formation of smaller-sized inclusions when grown at 30°C, although at this stage there is no evidence for this possibility.

When the solubilized protoxins were treated with trypsin, it yielded two major trypsin-resistant bands of 47 and ca. 20 kDa and some minor bands of about 40 kDa (see **Fig. 28, lane 3**). Thus, attempts have been tried to achieve complete activation by either optimizing the incubation time or varying the trypsin-protoxin ratio, but these minor bands were still observed. Therefore, N-terminal sequencing would be useful to identify undesirable trypsin digestion products. Yamagiwa et al (82) performed *in vivo* processing of Cry4A. They found that the Cry4A protoxin was processed into two

protease-resistant fragments of 20 and 45 kDa together with a band of about 40 kDa.

To determine the existence of the disulphide bond, gel-shift assays were employed. Based on the fact that the protein containing the disulphide bonds will have mobility faster than the one lacking the disulphide bond under non-reducing conditions. When the activated wild type toxins were analysed on non-reducing conditions via SDS-PAGE, it was found that the 20-kDa fragment, which is composed of α1-α5, treated with β-mercaptoethanol had mobility slower than the untreated protein (**Fig. 28, lanes 2-3**), suggesting the existence of the C192-C199 disulphide bond within the loop connecting α4 and α5 of the Cry4A toxin. It was also found that there is the mobility shift of ca. 40-kDa fragment (**Fig. 28, lanes 2-3**). There is no clear explanation for this observation, but this might be due to the formation of either an intramolecular disulphide bond in the 40 kDa protein or intermolecular disulphide bond of the 20-kDa fragments. Again, there is no evidence for this suggestion.

Further experiment is needed to confirm that the disulphide bond was not formed during proteolytic activation by using iodoacetamide which can irreversibly react with free thiol group preventing disulphide bond formation. However, this experiment is not trivial because iodoacetamide can also react with a histidine residue, although much less rapidly (83). The problem could be solved by incubating the solubilized protoxin with iodoacetamide in a short period of time followed by dialysis to prevent nonspecific reaction.

To investigate the role in toxicity of the disulphide bond within the interhelical loop, site-directed mutagenesis was employed to convert either Cys-192 or Cys-199 to alanine in order to eliminate the disulphide bond. Like the wild type protein, the

non-disulphide bridged mutants were highly expressed as inclusion bodies and were structurally stable upon solubilization and trypsin activation, suggested that they had folded correctly. Furthermore, gel-shift assays confirmed disappearance of the pre-existent disulphide bond (see **Fig. 36**).

For bioassays, either *E. coli* whole cells or inclusions was used to test for mosquito larvicidal activity. The larvicidal activity tested by feeding with *E. coli* whole cells expressing either non-disulphide bridged mutant exhibited approximately the same level as the wild type at three different cell concentrations (10^8-10^6 cells/ml). The differences in toxicity between the wild type and mutants could not be observed. Since the bioassays tested with *E. coli* whole cells had the limitation in determining toxin concentrations, the toxicity assay tested with 2 μg of inclusions would be another method to overcome this problem. The small (ca. 2 folds) but reproducible difference in larvicidal activity between the wild type inclusions and both mutant inclusions suggests that this disulphide bridge linking the α4-α5 loop might indeed be involved in Cry4A toxin function, possibly in promoting the helical hairpin's ability to translocate into the membrane interior. Accordingly by eliminating this stabilizing bond within the hairpin loop, it may be possible to reduce the effectiveness, even not much, of the mutant toxins by making the inserting hairpin less penetrable. However, it should be noted that the disulphide bond within the interhelical loop may not be existed in the 130-kDa protoxin, eventhough the existence of the disulphide bridge linking the α4-α5 loop was observed in the 20-kDa fragment of the activated toxin. Another caution here that applies to results with toxin inclusions is the possibility that the size of mutant inclusions might be smaller than the wild type inclusions. Since the *A. aegypti* larvae behave a collecting-filtering mode (84), the smaller mutant

inclusions could be filtered out by the larvae. To test this hypothesis, the size of both wild type and mutant inclusions could be verified by transmission electron microscopy. Dahl et al (85) found that the particle size which can be ingested by the larvae is ranging from 0.56-5.75 μm.

In vivo bioassays are not a sensitive technique and give only the limited information in toxicity. Moreover, there are several factors involved in the deviation of the results such as expression level, particle size and feeding behavior. Therefore, further functional investigation of the non-disulphide bridged mutants by using more sensitive assays such as *in vitro* toxicity or liposome assays needs to be carried out.

CHAPTER VII

CONCLUSION

1. The recombinant plasmid (pMEx-B4A) harboring the *cry4A* gene under control of the *tac* promoter together with the *cry4B* regulatory region was successfully constructed and highly expressed in *E. coli* upon IPTG induction as a cytoplasmic inclusion.

2. The Cry4A inclusions obtained from 10-hr IPTG induced *E.coli* containing pMEx-B4A grown at 30°C were able to be solubilized in carbonate buffer, pH 9.0.

3. The existence of the disulphide bond in the loop connecting α4 and α5 of the Cry4A toxin was determined by gel-shift assays.

4. The two non-disulphide bridged mutant plasmids (pC192A and pC199A) were successfully generated via site-directed mutagenesis using pMEx-B4A as a template.

5. The Cry4A mutants were highly expressed in the form of inclusion bodies and structurally stable upon solubilization and trypsin activation as the wild type toxin.

6. The larvicidal activity tested by feeding with *E. coli* whole cells expression either non-disulphide bridged mutant exhibited approximately the same level as the wild type at three different cell concentrations (10^8-10^6 cells/ml).

7. The larvicidal activity of wild type inclusions was apparently ca. 2-fold more toxic than both mutant inclusions.

REFERENCES

1. Schnepf E, Crickmore N, Van Rie J, Lereclus D, Baum J, Feitelson J, Zeigler DR, Dean DH. *Bacillus thuringiensis* and its pesticidal crystal proteins. Microbiol Mol Biol Rev 1998;62(3):775-806.
2. Aronson AI, Beckman W, Dunn P. *Bacillus thuringiensis* and related insect pathogens. Microbiol Rev 1986;50(1):1-24.
3. Hofte H, Whiteley HR. Insecticidal crystal proteins of *Bacillus thuringiensis*. Microbiol Rev 1989;53(2):242-255.
4. Feitelson JS, Payne J, Kim L. *Bacillus thuringiensis*: insects and beyond. Bio/Technology 1992;10:271-275.
5. Knowles BH. Mechanism of action of *Bacillus thuringiensis* insecticidal δ-endotoxin. Adv Insect Physiol 1994;24:276-307.
6. Crickmore N, Zeigler DR, Feitelson J, Schnepf E, Van Rie J, Lereclus D, Baum J, Dean DH. Revision of the nomenclature for the *Bacillus thuringiensis* pesticidal crystal proteins. Microbiol Mol Biol Rev 1998;62(3):807-813.
7. Ward ES, Ellar DJ. Nucleotide sequence of a *Bacillus thuringiensis* var. *israelensis* gene encoding a 130 kDa delta-endotoxin. Nucl Acids Res 1987;15:7195.
8. Li J, Carroll J, Ellar DJ. Crystal structure of insecticidal delta-endotoxin from *Bacillus thuringiensis* at 2.5 A° resolution. Nature 1991;353(6347):815-821.

9. Grochulski P, Masson L, Borisova S, Pusztai-Carey M, Schwartz JL, Brousseau R, Cygler M. *Bacillus thuringiensis* CryIA(a) insecticidal toxin: crystal structure and channel formation. J Mol Biol 1995;254(3):447-464.

10. Ahmad W, Ellar DJ. Directed mutagenesis of selected regions of a *Bacillus thuringiensis* entomocidal protein. FEMS Microbiol Lett 1990;56(1-2):97-104.

11. Wu D, Aronson AI. Localized mutagenesis defines regions of the *Bacillus thuringiensis* delta-endotoxin involved in toxicity and specificity. J Biol Chem 1992;267(4):2311-2317.

12. Chen XJ, Curtiss A, Alcantara E, Dean DH. Mutations in domain I of *Bacillus thuringiensis* delta-endotoxin CryIAb reduce the irreversible binding of toxin to *Manduca sexta* brush border membrane vesicles. J Biol Chem 1995;270(11):6412-6419.

13. Dean DH, Rajamohan F, Lee MK, Wu SJ, Chen XJ, Alcantara E, Hussain SR. Probing the mechanism of action of *Bacillus thuringiensis* insecticidal proteins by site-directed mutagenesis. Gene 1996;179(1):111-117.

14. Schwartz JL, Juteau M, Grochulski P, Cygler M, Prefontaine G, Brousseau R, Masson L. Restriction of intramolecular movements within the Cry1Aa toxin molecule of *Bacillus thuringiensis* through disulfide bond engineering. FEBS Lett 1997;410(2-3):397-402.

15. Gazit E, La Rocca P, Sansom MS, Shai Y. The structure and organization within the membrane of the helices composing the pore-forming domain of *Bacillus thuringiensis* delta-endotoxin are consistent with an "umbrella-

like" structure of the pore. Proc Natl Acad Sci U S A 1998;95(21):12289-12294.

16. Schnepf HE, Tomczak K, Ortega JP, Whiteley HR. Specificity-determining regions of a lepidopteran-specific insecticidal protein produced by *Bacillus thuringiensis*. J Biol Chem 1990;265(34):20923-20930.

17. Ge AZ, Rivers D, Milne R, Dean DH. Functional domains of *Bacillus thuringiensis* insecticidal crystal proteins. Refinement of *Heliothis virescens* and *Trichoplusia ni* specificity domains on CryIA(c). J Biol Chem 1991;266(27):17954-17958.

18. Smith GP, Ellar DJ. Mutagenesis of two surface-exposed loops of the *Bacillus thuringiensis* Cry1C δ-endotoxin affects insecticidal specificity. Biochem J 1994;302:611-616.

19. Lu H, Rajamohan F, Dean DH. Identification of amino acid residues of *Bacillus thuringiensis* delta-endotoxin CryIAa associated with membrane binding and toxicity to *Bombyx mori*. J Bacteriol 1994;176(17):5554-5559.

20. Wu SJ, Dean DH. Functional significance of loops in the receptor binding domain of *Bacillus thuringiensis* CryIIIA delta-endotoxin. J Mol Biol 1996;255 (4):628-640.

21. Smedley DP, Ellar DJ. Mutagenesis of three surface-exposed loops of a *Bacillus thuringiensis* insecticidal toxin reveals residues important for toxicity, receptor recognition and possibly membrane insertion. Microbiology 1996;142 (Pt 7):1617-1624.

22. Rajamohan F, Alcantara E, Lee MK, Chen XJ, Curtiss A, Dean DH. Single amino acid changes in domain II of *Bacillus thuringiensis* CryIAb delta-endotoxin affect irreversible binding to *Manduca sexta* midgut membrane vesicles. J Bacteriol 1995;177(9):2276-2282.

23. Rajamohan F, Cotrill JA, Gould F, Dean DH. Role of domain II, loop 2 residues of *Bacillus thuringiensis* CryIAb delta-endotoxin in reversible and irreversible binding to *Manduca sexta* and *Heliothis virescens*. J Biol Chem 1996;271(5):2390-2396.

24. Rajamohan F, Alzate O, Cotrill JA, Curtiss A, Dean DH. Protein engineering of *Bacillus thuringiensis* delta-endotoxin: mutations at domain II of CryIAb enhance receptor affinity and toxicity toward gypsy moth larvae. Proc Natl Acad Sci U S A 1996;93(25):14338-14343.

25. Rajamohan F, Hussain SRA, Cotrill JA, Gould F, Dean DH. Mutations at domain II, loop 3, of *Bacillus thuringiensis* CryIAa and CryIAb delta-endotoxins suggest loop 3 is involved in initial binding to lepidopteran midguts. J Biol Chem 1996;271(41):25220-25226.

26. Rajamohan F, Lee MK, Dean DH. *Bacillus thuringiensis* insecticidal proteins molecular mode of action. Progress in Nucleic Acids Research and Molecular Biology vol. 60. New York: Academic Press, 1998.

27. Chen XJ, Lee MK, Dean DH. Site-directed mutations in a highly conserved region of *Bacillus thuringiensis* delta-endotoxin affect inhibition of short circuit current across *Bombyx mori* midguts. Proc Natl Acad Sci U S A 1993;90 (19):9041-9045.

28. Wolfersberger MG, Chen XJ, Dean DH. Site-directed mutations in the third domain of *Bacillus thuringiensis* delta-endotoxin CryIAa affect its ability to increase the permeability of *Bombyx mori* midgut brush border membrane vesicles. Appl Environ Microbiol 1996;62(1):279-282.

29. Schwartz JL, Potvin L, Chen XJ, Brousseau R, Laprade R, Dean DH. Single-site mutations in the conserved alternating-arginine region affect ionic channels formed by CryIAa, a *Bacillus thuringiensis* toxin. Appl Environ Microbiol 1997;63(10):3978-3984.

30. Aronson AI Wu D, Zhang C. Mutagenesis of specificity and toxicity region of a *Bacillus thuringiensis* protoxin. J Biol Chem 1995;177:4059-4065.

31. de Maagd RA, Kwa MS, van der Klei H, Yamamoto T, Schipper B, Vlak JM, Stiekema WJ, Bosch D. Domain III substitution in *Bacillus thuringiensis* delta-endotoxin CryIA(b) results in superior toxicity for *Spodoptera exigua* and altered membrane protein recognition. Appl Environ Microbiol 1996;62(5):1537-1543.

32. de Maagd RA, van der Klei H, Bakker PL, Stiekema WJ, Bosch D. Different domains of *Bacillus thuringiensis* delta-endotoxins can bind to insect midgut membrane proteins on ligand blots. Appl Environ Microbiol 1996;62(8):2753-2757.

33. de Maagd RA, Bakker PL, Masson L, Adang MJ, Sangadala S, Stiekema W, Bosch D. Domain III of the *Bacillus thuringiensis* delta-endotoxin Cry1Ac is involved in binding to *Manduca sexta* brush border membranes and to its purified aminopeptidase N. Mol Microbiol 1999;31(2):463-471.

34. de Maagd RA, Bakker PL, Staykov N, Dukiandjiev S, Stiekema W, Bosch D. Identification of *Bacillus thuringiensis* delta-endotoxin Cry1C domain III amino acid residues involved in insect specificity. Appl Environ Microbiol 1999;65(10):4369-4374.

35. de Maagd RA,Hendriks MW, Stiekema W, Bosch D. *Bacillus thuringiensis* delta-endotoxin Cry1C domain III can function as a specificity determinant for *Spodoptera exigua* in different, but not all Cry1-Cry1C Hybrids. Appl Environ Microbiol 2000;66(4):1559-1563.

36. Lee MK, Milne RE, Ge AZ, Dean DH. Location of a *Bombyx mori* receptor binding region on a *Bacillus thuringiensis* delta-endotoxin. J Biol Chem 1992;267(5):3115-3121.

37. Lee MK, Young BA, Dean DH. Domain III exchanges of *Bacillus thuringiensis* CryIA toxins affect binding to different gypsy moth midgut receptors. Biochem Biophys Res Commun 1995;216(1):306-312.

38. Lee MK, You TH. Gould FL, Dean DH. Identification of residues in domain III of *Bacillus thuringiensis* Cry1Ac toxin that affect binding and toxicity. Appl Environ Microbiol 1999;65(10):4513-4520.

39. Burton SL, Ellar DJ, Li J, Derbyshire DJ. *N*-Acetylgalactosamine on the putative insect receptor aminopeptidase N is recognized by a site on the domain III lectin-like fold of a *Bacillus thuringiensis* insecticidal toxin. J Mol Biol 1999;287:1011-1022.

40. Uawithya P, Leetacheva S, Katzenmeier G, Panyim S, Krittanai C, Angsuthanasombat C. 3D Models for *Bacillus thuringiensis* Cry4A and

Cry4B insecticidal proteins based on homology modelling. Abst 32nd Meeting, Society for Invertebrate Pathology, Irvine, USA, 1999.

41. Aronson AI, Beckman W, Dunn P. *Bacillus thuringiensis* and related insect pathogens. Microbiol Rev 1986;50(1):1-24.

42. Angsuthanasombat C, Crickmore N, Ellar DJ. Cytotoxicity of a cloned *Bacillus thuringiensis* subsp. israelensis CryIVB toxin to an Aedes aegypti cell line. FEMS Microbiol Lett 1991;83:273-276.

43. Angsuthanasombat C, Crickmore N, Ellar DJ. Comparison of *Bacillus thuringiensis* subsp. *israelensis* CryIVA and CryIVB cloned toxins reveals synergism *in vivo*. FEMS Microbiol Lett 1992;94:63-68.

44. Prieto-Samsonov DL, Vazquez-Padron RI, Ayra-Pardo C, Gonzalez-Cabrera J, de la Riva GA. *Bacillus thuringiensis*: from biodiversity to biotechnology. J Ind Microbiol Biotechnol 1997;19(3):202-219.

45. Hofmann C, Vanderbruggen H, Hofte H, Van Rie J, Jansens S, Van Mellaert H. Specificity of *Bacillus thuringiensis* delta-endotoxins is correlated with the presence of high-affinity binding sites in the brush border membrane of target insect midguts. Proc Natl Acad Sci USA 1988;85:7844-7848.

46. Van Rie J, Jansens S, Hofte H, Degheele D, Van Mellaert H. Specificity of *Bacillus thuringiensis* δ-endotoxins: importance of specific receptors on the brush border membrane of the midgut of target insects. Eur J Biochem 1989;186:239-247.

47. Knight PJK, Crickmore N, Ellar DJ. The receptor for *Bacillus thuringiensis* Cry1A (c) delta-endotoxin in the brush border membrane of the lepidopteran *Manduca sexta* is aminopeptidase N. Mol Microbiol 1994;11:429-436.

48. Valaitis AP, Lee MK, Rajamohan F, Dean DH. Brush border membrane aminopeptidase-N in the midgut of the gypsy moth serves as the receptor for the Cry1A(c) δ-endotoxin of *Bacillus thuringiensis*. Insect Biochem Mol Biol 1995;25(10):1143-1151.

49. Gill SS, Cowles EA, Francis V. Identification, isolation, and cloning of a *Bacillus thuringiensis* CryIAc toxin-binding protein from the midgut of the lepidopteran insect *Heliothis virescens*. J Bio Chem 1995;270(45):27227-27282.

50. Denolf P, Hendrickx K, Van Damme J, Jansens S, Peferoen M, Degheele D, Van Rie J. Cloning and characterization of *Manduca sexta* and *Plutella xylostella* midgut aminopeptidase N enzymes related to *Bacillus thuringiensis* toxin binding proteins. Eur J Biochem 1997;248:748-761.

51. Vadlamudi RK, Weber E, Ji I, Ji TH, Bulla LA Jr. Cloning and expression of a receptor for an insecticidal toxin of *Bacillus thuringiensis*. J Biol Chem 1995;270(10):5490-5494.

52. Knowles BH, Ellar DJ. Colloid-osmotic lysis is a general feature of the mechanism of action of *Bacillus thuringiensis* δ-endotoxins with different insect specificity. Biochim Biophys Acta 1987;924:509-518.

53. Pietrantonio PV, Gill SS. *Bacillus thuringiensis* endotoxins: action on the insect midgut. In: Lchane MJ, Billingsley PF, editor. Biology of the Insect Midgut. London: Chapman and Hall, 1996:345-372.

54. Feng Q, Becktel WJ. pH-induced conformational transitions of Cry IA(a), Cry IA (c), and Cry IIIA delta-endotoxins in *Bacillus thuringiensis*. Biochemistry 1994;33(28):8521-8526.

55. Guereca L, Bravo A. The oligomeric state of *Bacillus thuringiensis* Cry toxins in solution. Biochim Biophys Acta 1999;1429(2):342-350.

56. Aronson AI, Geng C, Wu L. Aggregation of *Bacillus thuringiensis* Cry1A toxins upon binding to target insect larval midgut vesicles. Appl Environ Microbiol 1999;65(6):2503-2507.

57. Lorence A, Darszon A, Diaz C, Lievano A, Quintero R, Bravo A. δ-endotoxins induce cation channel in *Spodoptera frugiperda* brush border membrane in suspension and in planar lipid bilayers. FEBS Lett 1995;360:217-222.

58. Harvey WR, Crawford DN, Eisen NS, Fernandes VF, Spaeth DD, Wolfersberger MG. The potassium impermeable apical membrane of insect epithelia: a target for development of safe pesticides. Mem Inst Oswaldo Cruz 1987;82 Suppl 3:29-34.

59. Peyronnet O, Vachon V, Brousseau R, Baines D, Schwartz JL, Laprade R. Effect of *Bacillus thuringiensis* toxins on the membrane potential of lepidopteran insect midgut cells. Appl Environ Microbiol 1997;63 (5):1679-1684.

60. Slatin SL, Abrams CK, English L. Delta-endotoxins form cation-selective channels in planar lipid bilayers. Biochem Biophys Res Commun 1990;169(2):765-772.

61. Schwartz JL, Lu YJ, Sohnlein P, Brousseau R, Laprade R, Masson L, Adang MJ. Ion channels formed in planar lipid bilayers by *Bacillus thuringiensis* toxins in the presence of *Manduca sexta* midgut receptors. FEBS Lett 1997;412(2):270-276.

62. Walters FS, Slatin SL, Kulesza CA, English LH. Ion channel activity of N-terminal fragments from CryIA(c) delta-endotoxin. Biochem Biophys Res Commun 1993;196(2):921-926.

63. Von Tersch MA, Slatin SL, Kulesza CA, English LH. Membrane-permeabilizing activities of *Bacillus thuringiensis* coleopteran-active toxin CryIIIB2 and CryIIIB2 domain I peptide. Appl Environ Microbiol 1994;60(10):3711-3717.

64. Uawithya P, Tuntitippawan T, Katzenmeier G, Panyim S, Angsuthanasombat C. Effects on larvicidal activity of single proline substitutions in alpha3 or alpha4 of the *Bacillus thuringiensis* Cry4B toxin. Biochem Mol Biol Int 1998;44(4):825-832.

65. Manoj Kumar AS, Aronson AI. Analysis of mutations in the pore-forming region essential for insecticidal activity of a *Bacillus thuringiensis* δ-endotoxin. J Bacteriol 1999;181(19):6103-6107.

66. Cummings CE, Armstrong G, Hodgman TC, Ellar DJ. Structural and functional studies of a synthetic peptide mimicking a proposed membrane inserting

region of a *Bacillus thuringiensis* delta-endotoxin. Mol Membr Biol 1994;11(2):87-92.

67. Gazit E, Shai Y. Structural and functional characterization of the alpha 5 segment of *Bacillus thuringiensis* delta-endotoxin. Biochemistry 1993;32 (13):3429-3436.

68. Gazit E, Shai Y. The assembly and organization of the alpha 5 and alpha 7 helices from the pore-forming domain of *Bacillus thuringiensis* delta-endotoxin. Relevance to a functional model. J Biol Chem 1995;270(6):2571-2578.

69. Gazit E, Bach D, Kerr ID, Sansom MS, Chejanovsky N, Shai Y. The alpha-5 segment of *Bacillus thuringiensis* delta-endotoxin: *in vitro* activity, ion channel formation and molecular modelling. Biochem J 1994;304 (Pt 3):895-902.

70. Piroonla-ong T. Functional studies of regulatory regions involved in expression of the 130 kDa Cry4 mosquito-larvicidal toxin gene in *Escherichia coli*. [M.S. Thesis in Molecular Genetics and Genetic Engineering]. Bangkok: Faculty of Graduate Studies, Mahidol University, 1998.

71. Buttcher V, Ruhlmann A, Cramer F. Improved single-stranded DNA producing expression vectors for protein manipulation in *Escherichia coli*. Nucl Acids Res 1990;18(4):1075-1078.

72. Sambrook J, Maniatis T, Fritsch EF. Molecular cloning: a laboratory manual. Cold Spring Harbor laboratory 1989.

73. Del Sal G, Manfioletti G, Schneider C. A one-tube plasmid DNA mini preparation suitable for sequencing. Nucl Acids Res 1988;16:9878.

74. Chen M, Christen P. Removal of chromosomal DNA by $Mg2^{+}$ in the lysis buffer: an improved lysis protocol for preparing *Escherichia coli* whole-cell lysates for sodium dodecyl sulfate-polyacrylamide gel electrophoresis. Anal Biochem 1997;246(2):263-264.

75. Laemmli UK, Molbert E, Showe M, Kellenberger E. Form-determining function of the genes required for the assembly of the head of bacteriophage T4. J Mol Biol 1970;49(1):99-113.

76. Angsuthanasombat C. Mechanism of action of *Bacillus thuringiensis* var. *israelensis* mosquito-larvicidal δ-endotoxins [Ph.D. Thesis in Biochemistry]. University of Cambridge, 1993.

77. Bradford MM. A rapid and sensitive method for the quantitation for microgram quantities of protein utilizing the principle of protein-dye binding. Anal Biochem 1976;72:248-254.

78. Gray WR. Disulphide bonds between cysteine residues. In: Creighton TE, editor. Protein Structure (A Practical Approach). 2nd ed. New York: Oxford University Press Inc, 1997:165-186.

79. Angsuthanasombat C, Chungjatupornchai W, Kertbundit S, Luxananil P, Settasatian C, Wilairat P, Panyim P. Cloning and expression of 130-kDa mosquito-larvicidal δ-endotoxin gene of *Bacillus thuringiensis* var. *israelensis* in *Escherichia coli*. Mol Gen Genet 1987;208:384-389.

80. Pao-intrara M. Structure-function relationship of the gene encoding 130-kDa-mosquito larvicidal protein. [M.S. Thesis in Biochemistry]. Bangkok: Faculty of Graduate Studies, Mahidol University, 1987.

81. Simons JFA, Boots JP, Slotboom AJ, Verheij HM. The (phospho)lipase from *Staphylococcus hyicus*: expression in *Escherichia coli*, large-scale purification and application in esterification reactions. J Mol Catalyst B: Enzymatic 1997;3(1-4):13-23.

82. Yamakiwa M, Esaki M, Otake K, Inagaki M, Komano T, Amachi T, Sakai H. Activation process of dipteran-specific insecticidal protein produced by *Bacillus thuringiensis* subsp. *israelensis*. Appl Environ Microbiol 1999;65(8):3464-3469.

83. Creighton TE. Proteins: Structures and Molecular properties. 2nd ed. New York: W.H. Freeman and Company, 1993.

84. Merritt RW, Dadd RH, Walker ED. Feeding behavior, natural food, and nutritional relationships of larval mosquitoes. Annu Rev Entomol 1992;37:349-376.

85. Dahl C, Sahlen G, Grawe J, Johannisson A, Amneus H. Different particle uptake by larvae of three mosquito species (Diptera: Culicidae). J Med Entomol 1993;30(3):537-543.

APPENDIX

Complete nucleotide sequence of *cry4A* gene

The nucleotide sequence shown is the sequence of *cry4A* gene in pBA. The uppercase letters represent the deduced amino acid sequence. The cysteine-192 and cysteine-199 are in bold type. The predicted alpha helices in domain I are marked as box.

```
atg aat cct tat caa aat aaa aat gaa tat gaa aca tta aat gct   45
 M   N   P   Y   Q   N   K   N   E   Y   E   T   L   N   A   15

tca caa aaa aaa tta aat ata tct aat aat tat aca aga tat cca   90
 S   Q   K   K   L   N   I   S   N   N   Y   T   R   Y   P   30

ata gaa aat agt cca aaa caa tta tta caa agt aca aat tat aaa   135
 I   E   N   S   P   K   Q   L   L   Q   S   T   N   Y   K   45

gat tgg ctc aat atg tgt caa cag aat cag cag tat ggt gga gat   180
 D   W   L   N   M   C   Q   Q   N   Q   Q   Y   G   G   D   60
                                  Helix 1
ttt gaa act ttt att gat agt ggt gaa ctc agt gcc tat act att   225
 F   E   T   F   I   D  S   G   E   L   S   A   Y   T   I   75

gta gtt ggg acc gta ctg act ggt ttc ggg ttc aca aca ccc tta   270
 V   V   G   T   V   L   T   G  F   G   F   T   T   P   L   90
                  Helix 2a
gga ctt gct tta ata ggt ttt ggt aca tta ata cca gtt ctt ttt   315
 G   L   A   L   I   G   F   G   T   L   I   P   V   L   F   105
                                  Helix 2b
cca gcc caa gac caa tct aac aca tgg agt gac ttt ata aca caa   360
 P   A   Q   D   Q   S  N   T   W   S   D   F   I   T   Q   120

act aaa aat att ata aaa aaa gaa ata gca tca aca tat ata agt   405
 T   K   N   I   I  K   K   E   I   A  S   T   Y   I   S   135
                  Helix 3
aat gct aat aaa att tta aac agg tcg ttt aat gtt atc agc act   450
 N   A   N   K   I   L   N   R   S   F   N   V   I   S   T   150

tat cat aat cac ctt aaa aca tgg gag aat aat cca aac cca caa   495
 Y   H   N   H   L   K   T   W   E   N  N   P   N   P   Q   165
                  Helix 4
aat act cag gat gta agg aca caa atc cag cta gtt cat tac cat   540
 N   T   Q   D   V   R   T   Q   I   Q   L   V   H   Y   H   180

ttt caa aat gtc att cca gag ctt gta aac tct tgt cct cct aat   585
 F   Q   N   V   I   P   E  L   V   N   S  C   P   P   N   195

cct agt gat tgc gat tac tat aac ata cta gta tta tct agt tat   630
 P   S   D  C   D   Y   Y   N   I   L  V   L   S   S   Y   210
                  Helix 5
gca caa gca gca aac tta cat ctg act gta tta aat caa gcc gtc   675
 A   Q   A   A   N   L   H   L   T   V   L   N   Q   A   V   225

aaa ttt gaa gcg tat tta aaa aac aat cga caa ttc gat tat tta   720
 K   F  E   A   Y   L   K   N   N   R   Q   F   D   Y   L   240

gag cct ttg cca aca gca att gat tat tat cca gta ttg act aaa   765
 E   P   L   P   T   A  I   D   Y   Y   P   V   L   T   K   255
```

Helix 6

```
gct ata gaa gat tac act aat tat tgt gta aca act tat aaa aaa  810
 A   I   E   D   Y   T   N   Y   C   V   T   T   Y   K   K   270

gga tta aat tta att aaa acg acg cct gat agt aat ctt gat gga  855
 G   L   N   L   I   K   T   T   P   D   S   N   L   D   G  285
```

Helix 7

```
aat ata aac tgg aac aca tac aat acg tat cga aca aaa atg act  900
 N   I   N   W   N   T   Y   N   T   Y   R   T   K   M   T  300

act gct gta tta gat gtt gtt gca ctc ttt cct aat tat gat gta  945
 T   A   V   L   D   V   V   A   L   F   P   N   Y   D   V  315

ggt aaa tat cca ata ggt gtc caa tct gaa ctt act cga gaa att  990
 G   K   Y   P   I   G   V   Q   S   E   L   T   R   E   I  330

tat cag gta ctt aac ttc gaa gaa agc ccc tat aaa tat tat gac 1035
 Y   Q   V   L   N   F   E   E   S   P   Y   K   Y   Y   D  345

ttt caa tat caa gag gat tca ctt aca cgt aga ccg cat tta ttt 1080
 F   Q   Y   Q   E   D   S   L   T   R   R   P   H   L   F  360

act tgg ctt gat tct ttg aat ttt tat gaa aaa gcg caa act act 1125
 T   W   L   D   S   L   N   F   Y   E   K   A   Q   T   T  375

cct aat aat ttt ttc acc agc cat tat aat atg ttt cat tac aca 1170
 P   N   N   F   F   T   S   H   Y   N   M   F   H   Y   T  390

ctt gat aat ata tcc caa aaa tct agt gtt ttt gga aat cac aat 1215
 L   D   N   I   S   Q   K   S   S   V   F   G   N   H   N  405

gta act gat aaa tta aaa tct ctt ggt ttg gca aca aat att tat 1260
 V   T   D   K   L   K   S   L   G   L   A   T   N   I   Y  420

att ttt tta tta aat gtc ata agc tta gat aat aaa tat cta aat 1305
 I   F   L   L   N   V   I   S   L   D   N   K   Y   L   N  435

gat tat aat aat att agt aaa atg gat ttt ttt ata act aat ggt 1350
 D   Y   N   N   I   S   K   M   D   F   F   I   T   N   G  450

act aga ctt ttg gag aaa gaa ctt aca gca gga tct ggg caa ata 1395
 T   R   L   L   E   K   E   L   T   A   G   S   G   Q   I  465

act tat gat gta aat aaa aat att ttc ggg tta cca att ctt aaa 1440
 T   Y   D   V   N   K   N   I   F   G   L   P   I   L   K  480

cga aga gag aat caa gga aac cct acc ctt ttt cca aca tat gat 1485
 R   R   E   N   Q   G   N   P   T   L   F   P   T   Y   D  495

aac tat agt cat att tta tca ttt att aaa agt ctt agt atc cct 1530
 N   Y   S   H   I   L   S   F   I   K   S   L   S   I   P  510

gca aca tat aaa act caa gtg tat acg ttt gct tgg aca cac tct 1575
 A   T   Y   K   T   Q   V   Y   T   F   A   W   T   H   S  525

agt gtt gat cct aaa aat aca att tat aca cat tta act acc caa 1620
 S   V   D   P   K   N   T   I   Y   T   H   L   T   T   Q  540

att cca gct gta aaa gcg aat tca ctt ggg act gct tct aag gtt 1665
 I   P   A   V   K   A   N   S   L   G   T   A   S   K   V  555

gtt caa gga cct ggt cat aca gga ggg gat tta att gat ttc aaa 1710
 V   Q   G   P   G   H   T   G   G   D   L   I   D   F   K  570
```

```
gat cat ttc aaa att aca tgt caa cac tca aat ttt caa caa tcg   1755
 D   H   F   K   I   T   C   Q   H   S   N   F   Q   Q   S    585

tat ttt ata aga att cgt tat gct tca aat gga agc gca aat act   1800
 Y   F   I   R   I   R   Y   A   S   N   G   S   A   N   T    600

cga gct gtt ata aat ctt agt atc cca ggg gta gca gaa ctg ggt   1845
 R   A   V   I   N   L   S   I   P   G   V   A   E   L   G    615

atg gca ctc aac ccc act ttt tct ggt aca gat tat acg aat tta   1890
 M   A   L   N   P   T   F   S   G   T   D   Y   T   N   L    630

aaa tat aaa gat ttt cag tac tta gaa ttt tct aac gag gtg aaa   1935
 K   Y   K   D   F   Q   Y   L   E   F   S   N   E   V   K    645

ttt gct cca aat caa aac ata tct ctt gtg ttt aat cgt tcg gat   1980
 F   A   P   N   Q   N   I   S   L   V   F   N   R   S   D    660

gta tat aca aac aca aca gta ctt att gat aaa att gaa ttt ctg   2025
 V   Y   T   N   T   T   V   L   I   D   K   I   E   F   L    675

cca att act cgt tct ata aga gag gat aga gag aaa caa aaa tta   2070
 P   I   T   R   S   I   R   E   D   R   E   K   Q   K   L    690

gaa aca gta caa caa ata att aat aca ttt tat gca aat cct ata   2115
 E   T   V   Q   Q   I   I   N   T   F   Y   A   N   P   I    705

aaa aac act tta caa tca gaa ctt aca gat tat gac ata gat caa   2160
 K   N   T   L   Q   S   E   L   T   D   Y   D   I   D   Q    720

gcc gca aat ctt gtg gaa tgt att tct gaa gaa tta tat cca aaa   2205
 A   A   N   L   V   E   C   I   S   E   E   L   Y   P   K    735

gaa aaa atg ctg tta tta gat gaa gtt aaa aat gcg aaa caa ctt   2250
 E   K   M   L   L   L   D   E   V   K   N   A   K   Q   L    750

agt caa tct cga aat gta ctt caa aac ggg gat ttt gaa tcg gct   2295
 S   Q   S   R   N   V   L   Q   N   G   D   F   E   S   A    765

acg ctt ggt tgg aca aca agt gat aat atc aca att caa gaa gat   2340
 T   L   G   W   T   T   S   D   N   I   T   I   Q   E   D    780

gat cct att ttt aaa ggg cat tac ctt cat atg tct ggg gcg aga   2385
 D   P   I   F   K   G   H   Y   L   H   M   S   G   A   R    795

gac att gat ggt acg ata ttt ccg acc tat ata ttc caa aaa att   2430
 D   I   D   G   T   I   F   P   T   Y   I   F   Q   K   I    810

gat gaa tca aaa tta aaa ccg tat aca cgt tac cta gta agg gga   2475
 D   E   S   K   L   K   P   Y   T   R   Y   L   V   R   G    825

ttt gta gga agt agt aaa gat gta gaa cta gtg gtt tca cgc tat   2520
 F   V   G   S   S   K   D   V   E   L   V   V   S   R   Y    840

ggg gaa gaa att gat gcc atc atg aat gtt cca gct gat tta aac   2565
 G   E   E   I   D   A   I   M   N   V   P   A   D   L   N    855

tat ctg tat cct tct acc ttt gat tgt gaa ggg tct aat cgt tgt   2610
 Y   L   Y   P   S   T   F   D   C   E   G   S   N   R   C    870

gag acg tcc gct gtg ccg gct aac att ggg aac act tct gat atg   2655
 E   T   S   A   V   P   A   N   I   G   N   T   S   D   M    885
```

```
ttg tat tca tgc caa tat gat aca ggg aaa aag cat gtc gta tgt   2700
 L   Y   S   C   Q   Y   D   T   G   K   K   H   V   V   C    900

cag gat tcc cat caa ttt agt ttc act att gat aca ggg gca tta   2745
 Q   D   S   H   Q   F   S   F   T   I   D   T   G   A   L    915

gat aca aat gaa aat ata ggg gtt tgg gtc atg ttt aaa ata tct   2790
 D   T   N   E   N   I   G   V   W   V   M   F   K   I   S    930

tct cca gat gga tac gca tca tta gat aat tta gaa gta att gaa   2835
 S   P   D   G   Y   A   S   L   D   N   L   E   V   I   E    945

gaa ggg cca ata gat ggg gaa gca ctg tca cgc gtg aaa cac atg   2880
 E   G   P   I   D   G   E   A   L   S   R   V   K   H   M    960

gag aag aaa tgg aac gat caa atg gaa gca aaa cgt tcg gaa aca   2925
 E   K   K   W   N   D   Q   M   E   A   K   R   S   E   T    975

caa caa gca tat gat gta gcg aaa caa gcc att gat gct tta ttc   2970
 Q   Q   A   Y   D   V   A   K   Q   A   I   D   A   L   F    990

aca aat gta caa gat gag gct tta cag ttt gat acg aca ctc gct   3015
 T   N   V   Q   D   E   A   L   Q   F   D   T   T   L   A   1005

caa att cag tac gct gag tat ttg gta caa tcg att cca tat gtg   3060
 Q   I   Q   Y   A   E   Y   L   V   Q   S   I   P   Y   V   1020

tac aat gat tgg ttg tca gat gtt cca ggt atg aat tat gat atc   3105
 Y   N   D   W   L   S   D   V   P   G   M   N   Y   D   I   1035

tat gta gag ttg gat gca cga gtg gca caa gcg cgt tat ttg tat   3150
 Y   V   E   L   D   A   R   V   A   Q   A   R   Y   L   Y   1050

gat ata aga aat att att aaa aat ggt gat ttt aca caa ggg gta   3195
 D   I   R   N   I   I   K   N   G   D   F   T   Q   G   V   1065

atg ggg tgg cat gta act gga aat gca gac gta caa caa ata gat   3240
 M   G   W   H   V   T   G   N   A   D   V   Q   Q   I   D   1080

ggt gtt tct gta ttg gtt cta tct aat tgg agt gct ggc gta tct   3285
 G   V   S   V   L   V   L   S   N   W   S   A   G   V   S   1095

caa aat gtc cat ctc caa cat aat cat ggg tat gtc tta ggt gtt   3330
 Q   N   V   H   L   Q   H   N   H   G   Y   V   L   G   V   1110

att gcc aaa aaa gaa gga cct gga aat ggg tat gtc acg ctt atg   3375
 I   A   K   K   E   G   P   G   N   G   Y   V   T   L   M   1125

gat tgg gag gag aat caa gaa aaa ttg acg ttt acg tct tgt gaa   3420
 D   W   E   E   N   Q   E   K   L   T   F   T   S   C   E   1140

gaa gga tat att acg aag aca gta gat gta ttc cca gat aca gat   3465
 E   G   Y   I   T   K   T   V   D   V   F   P   D   T   D   1155

cgt gta cga att gag ata ggc gaa acc gaa ggt tcg ttt tat atc   3510
 R   V   R   I   E   I   G   E   T   E   G   S   F   Y   I   1170

gaa agc att gaa tta att tgc atg aac gag                      3540
 E   S   I   E   L   I   C   M   N   E                       1180
```

BIOGRAPHY

NAME Ms. Walairat Pornwiroon

DATE OF BIRTH 21 May 1975

PLACE OF BIRTH Bangkok, Thailand

INSTITUTIONS ATTENDED

Kasetsart University, 1993-1996:
Bachelor of Science (Biotechnology)

Mahidol University, 1998-2000:
Master of Science (Molecular Genetics-Genetic Engineering)

RESEARCH GRANTS

Thailand Research Fund's Research Fellowships granted to Professor Sakol Panyim